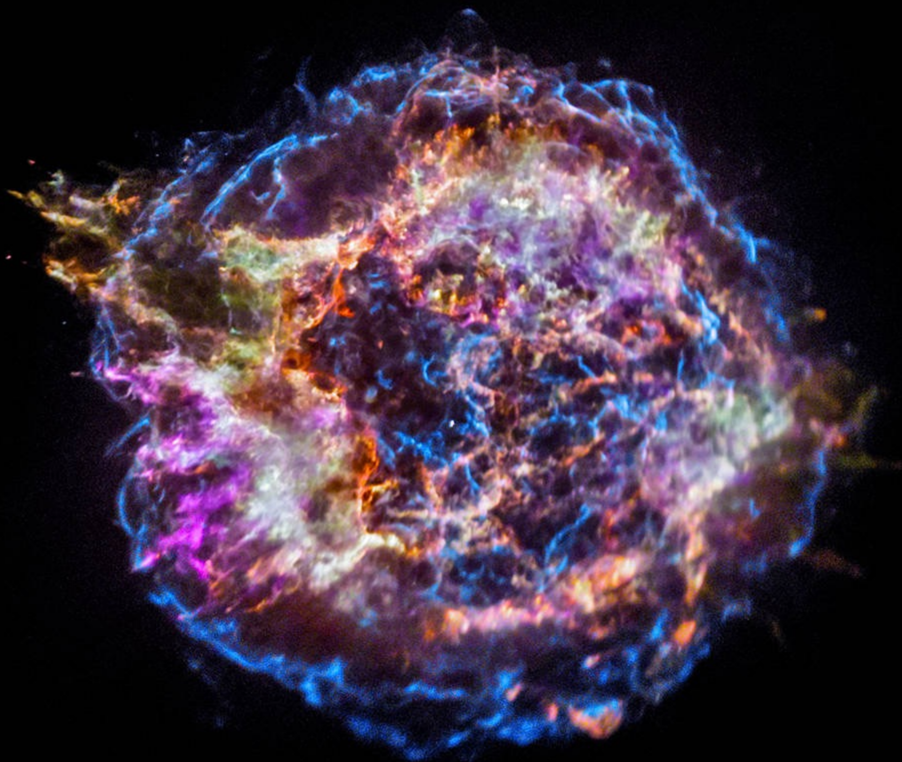

Interplay of waves and vorticity in the shallow water analogue of a collapsing stellar core

Thierry Foglizzo

CEA Saclay

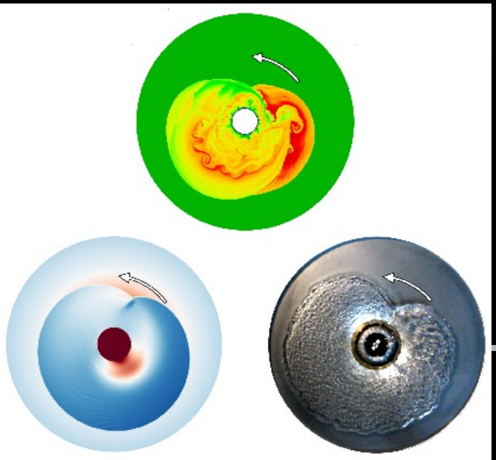

G. Durand, J. Guilet, M. González, F. Masset
L. Walk, I. Tamborra (U. Copenhagen)

Outline

Astrophysics background

Experiment and St Venant model
- Experimental setup
- Idealized St Venant model
- Comparing the model to the experiment

Physical understanding of linear processes
- Instability mechanism
- Slower growth in the experiment
- Destabilizing effect of rotation

Non linear challenges
- Saturation mechanism
- Impact of turbulence
- Surfing optimization

Benefits for astrophysics

Astrophysics background in 47s Youtube/CEA "How does a supernova explode?" (6mn)

Theoretical framework (Bethe & Wilson 85)
neutrino-driven delayed explosion

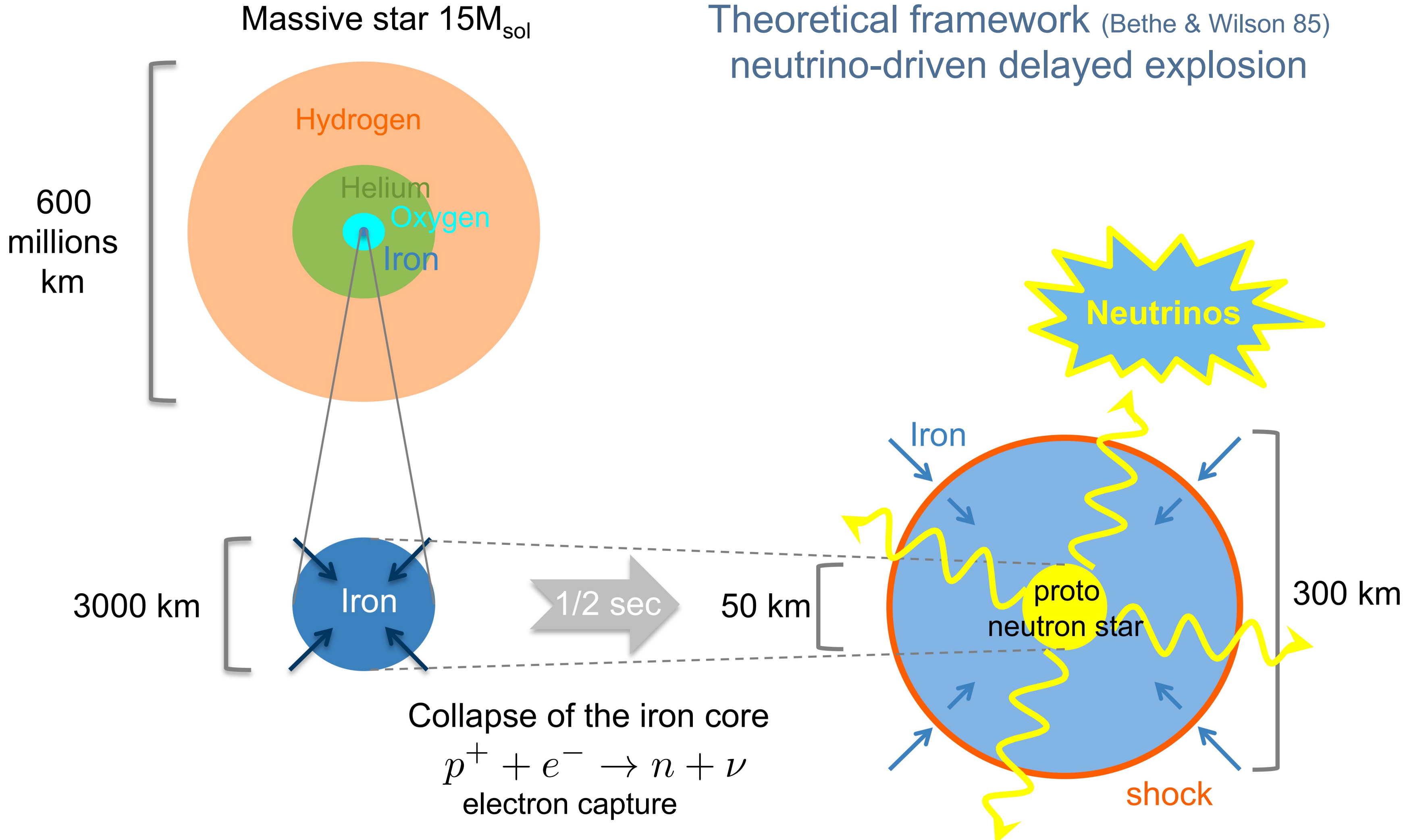

$$\frac{GM_{\rm ns}^2}{R_{\rm ns}} \sim 2\times 10^{53}{\rm erg}\left(\frac{30{\rm km}}{R_{\rm ns}}\right)\left(\frac{M_{\rm ns}}{1.5M_{\rm sol}}\right)^2$$

---

modest energy in differential rotation: $E_{\rm diff} < E_{\rm rot} \sim 2.4\times 10^{50}{\rm erg}\left(\frac{M_{\rm ns}}{1.5M_{\rm sol}}\right)\left(\frac{R_{\rm ns}}{10{\rm km}}\right)^2\left(\frac{10{\rm ms}}{P_{\rm ns}}\right)^2$

$27M_{sol}$ stellar core collapse in 3D

Hanke et al. 13

time evolution: 500ms
diameter: 300km

PRACE
150 million hours
16.000 processors
4.5 months/model

2 instabilities during the phase of stalled accretion shock

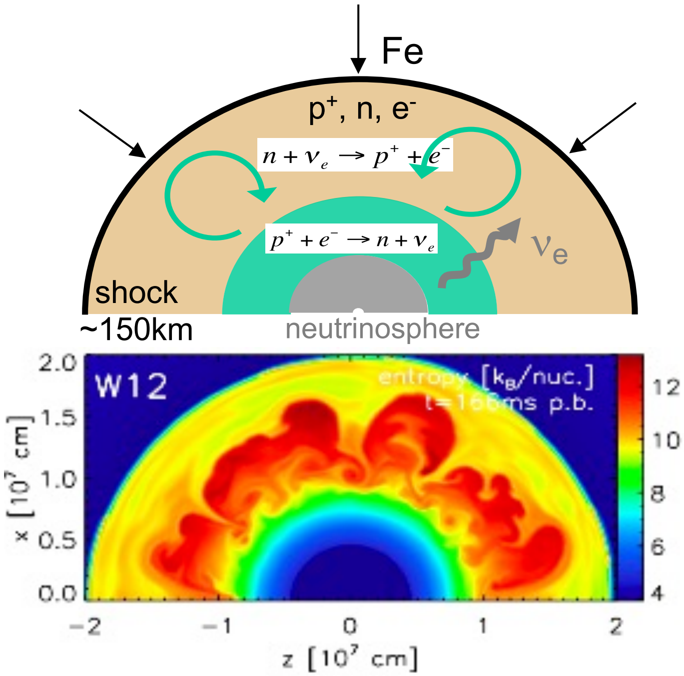

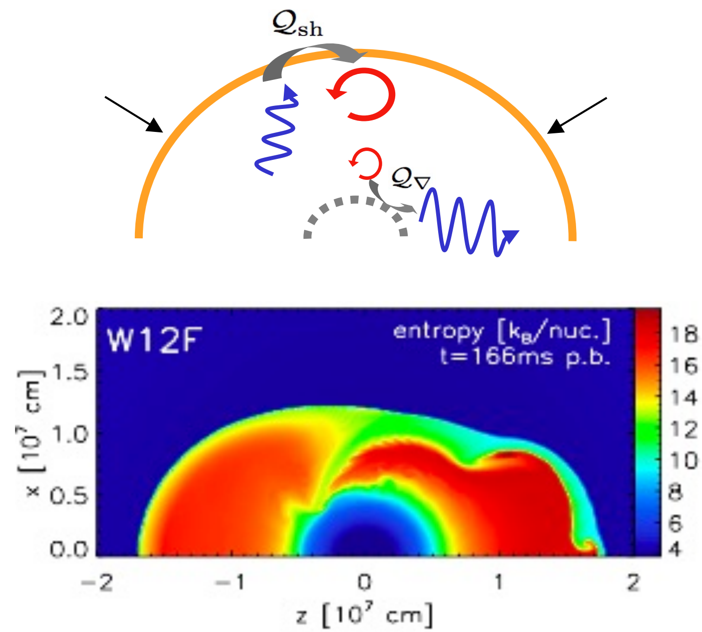

Neutrino-driven convection

(Herant+92)

- entropy gradient
- angular scale l=5,6

SASI: Standing Accretion Shock Instability

(Blondin+03)

- advective-acoustic cycle
- oscillatory, large angular scale l=1,2

Supernovae as laboratories of extreme physics

+ Physical modeling with approximate numerical simulations

  - Newtonian gravity + special relativity + general relativity
  - 3D compressible hydro + turbulence + MHD + dynamo
  - Neutrino interactions and transport in 7D (x,y,z,E,θ,φ,t)
  - Equation of State at nuclear density
  - Exotic physics (quark matter, sterile neutrino, axions ...)

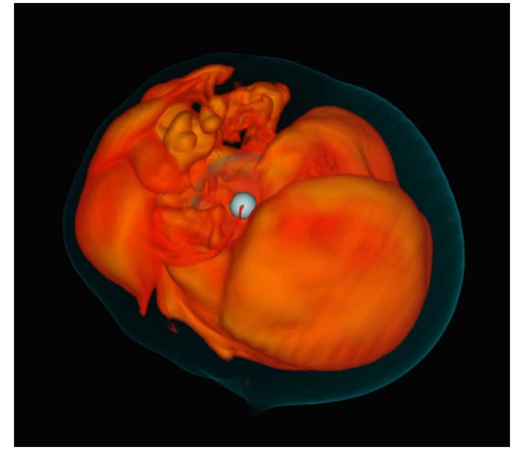

Hanke+13

+ Observations of

  -neutrinos & gravitational waves,
  -light curve at all electromagnetic frequencies,
  -remnant composition,
  -neutron stars and black holes properties (mass, kick, spin)

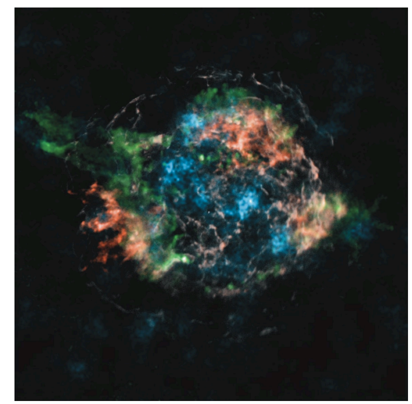

Grefenstette+14

+ Analogue experiment
  -2-3D hydrodynamics
  -gravity
  -turbulence

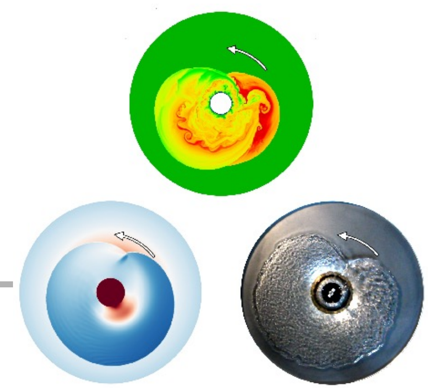

Outline

Astrophysics background

Experiment and St Venant model
- Experimental setup
- Idealized St Venant model
- Comparing the model to the experiment

Physical understanding of linear processes
- Instability mechanism
- Slower growth in the experiment
- Destabilizing effect of rotation

Non linear challenges
- Saturation mechanism
- Impact of turbulence
- Surfing optimization

Benefits for astrophysics

Hydraulic jumps and shock waves

Hydraulic jumps and shock waves

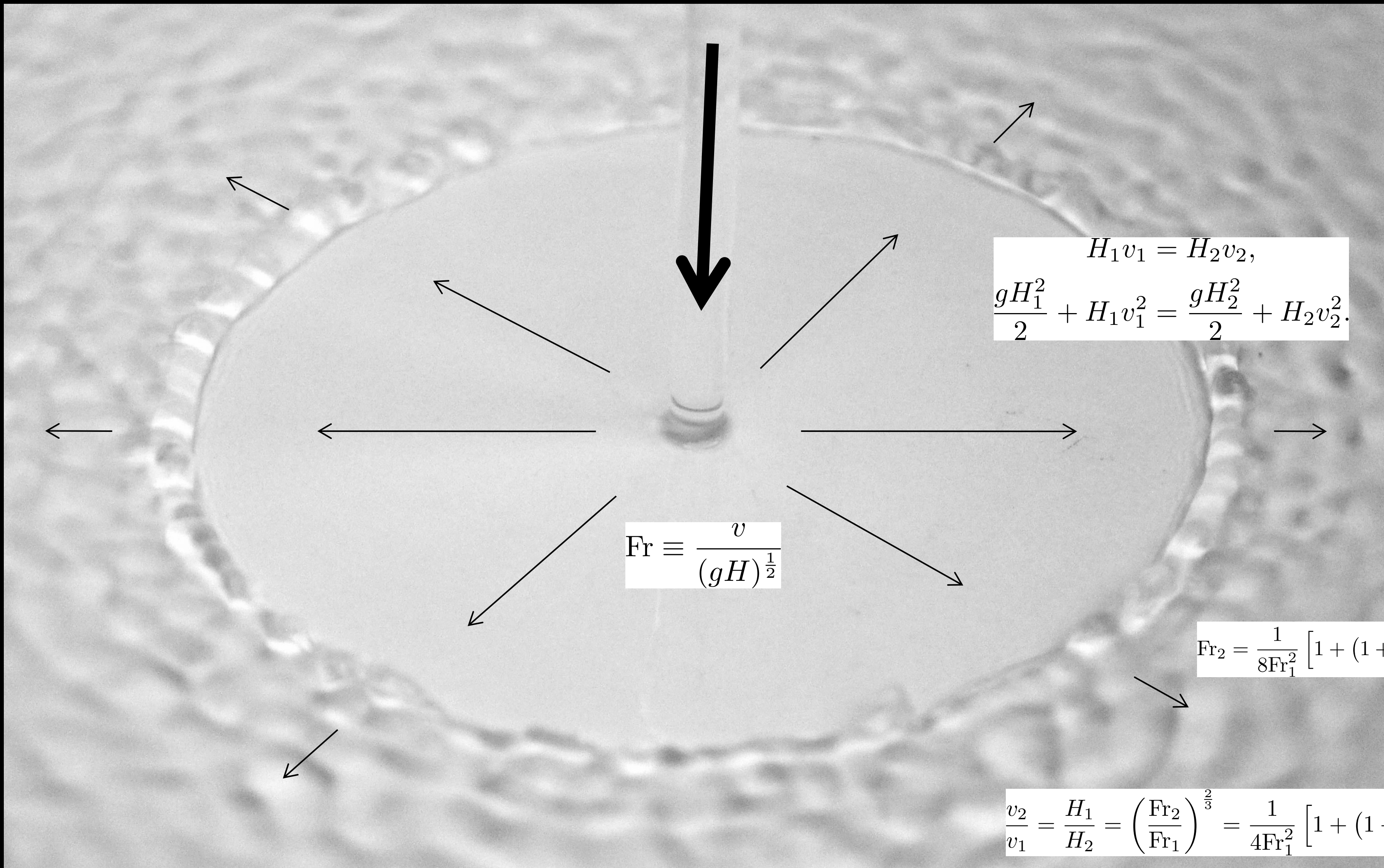

$$H_1 v_1 = H_2 v_2,$$
$$\frac{gH_1^2}{2} + H_1 v_1^2 = \frac{gH_2^2}{2} + H_2 v_2^2.$$

$$\mathrm{Fr} \equiv \frac{v}{(gH)^{\frac{1}{2}}}$$

$$\mathrm{Fr}_2 = \frac{1}{8\mathrm{Fr}_1^2}\left[1 + \left(1 + 8\mathrm{Fr}_1^2\right)^{\frac{1}{2}}\right]^{\frac{3}{2}}$$

$$\frac{v_2}{v_1} = \frac{H_1}{H_2} = \left(\frac{\mathrm{Fr}_2}{\mathrm{Fr}_1}\right)^{\frac{2}{3}} = \frac{1}{4\mathrm{Fr}_1^2}\left[1 + \left(1 + 8\mathrm{Fr}_1^2\right)^{\frac{1}{2}}\right]$$

Analogy between hydraulic jumps and shock

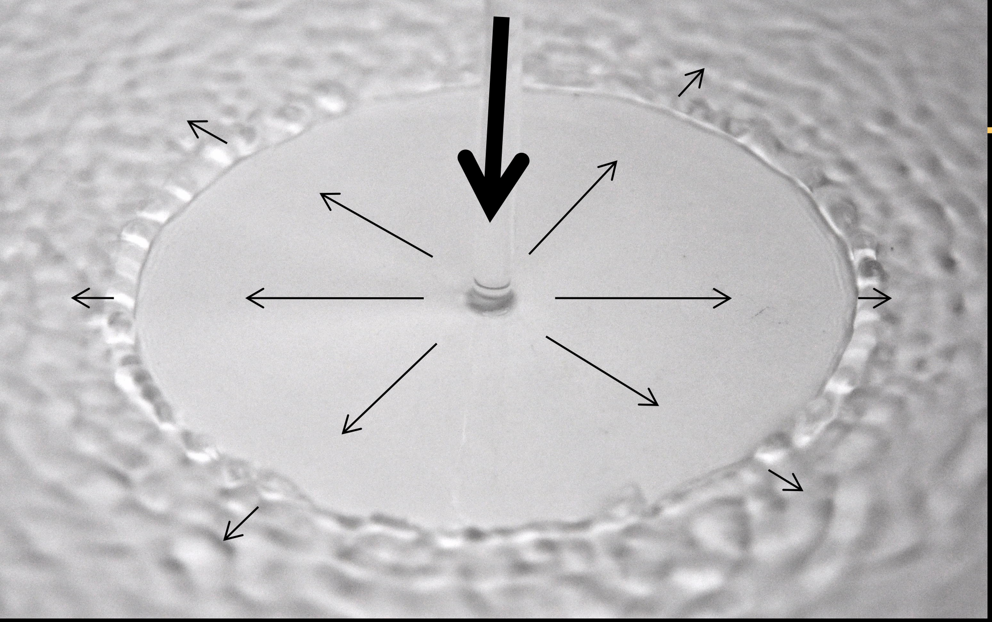

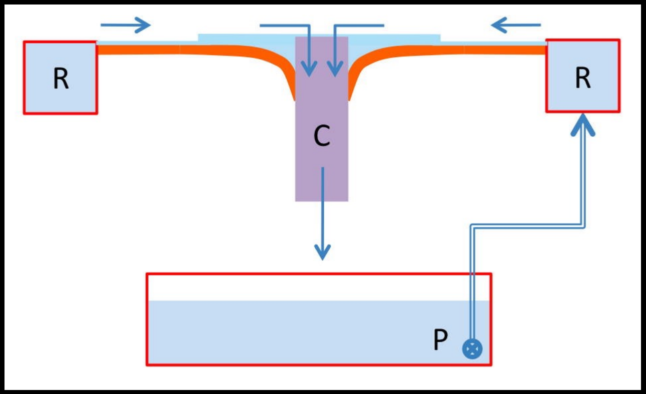

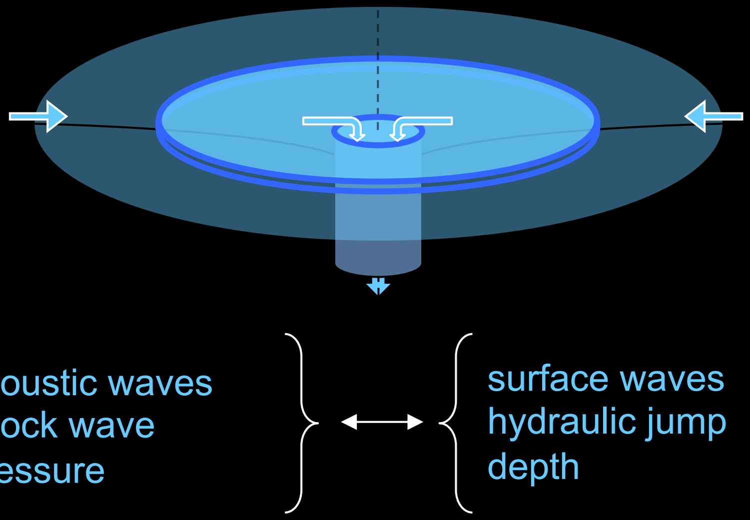

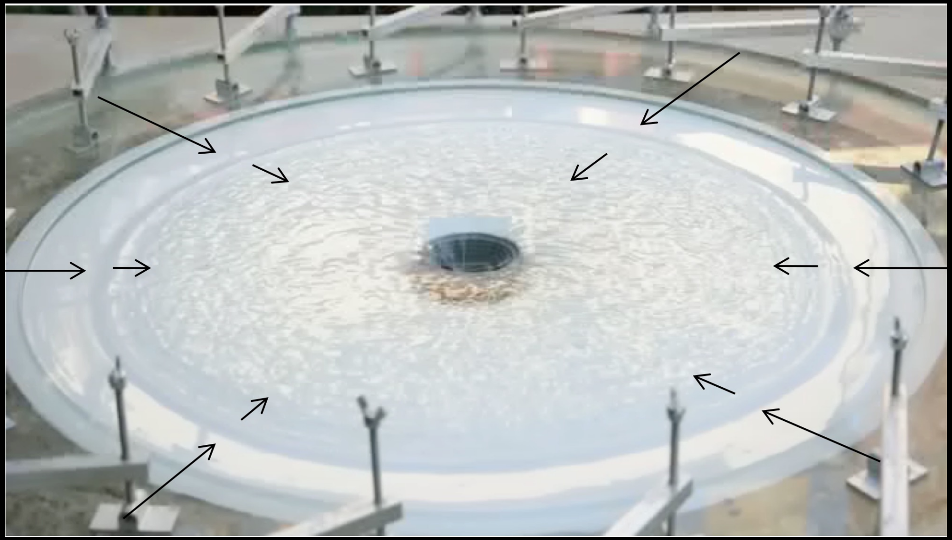

SWASI: simple as a garden experiment

November 2010

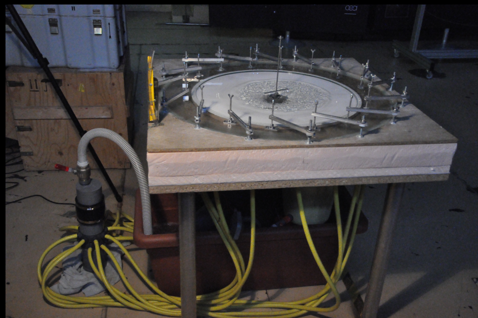

October 2010

June 2010

May 2010

February 2012

Nov-Dec. 2013 & since 2015:
Palais de la Découverte, Paris

PRIX 2014
LE GOÛT
DES SCIENCES

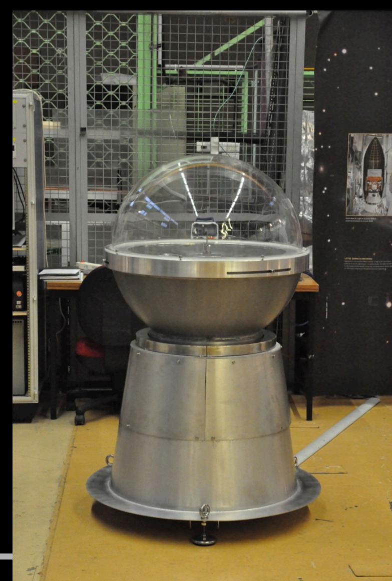

June 2014

February 2017

+ Gilles Durand

Mai 2021

Dynamics of water
in the fountain

Dynamics of the gas
in the supernova core

diameter 40cm ← 1 000 000 x bigger → diameter 400km

3s/oscillation ← 100 x faster → 0.03s/oscillation

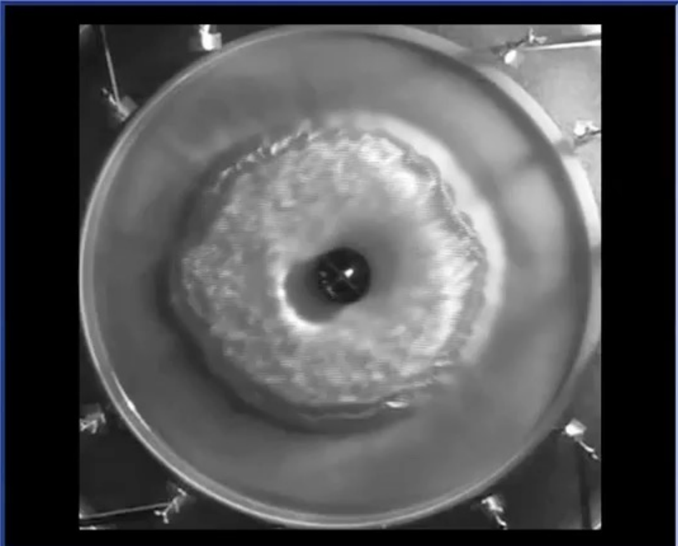

Expérience hydraulique

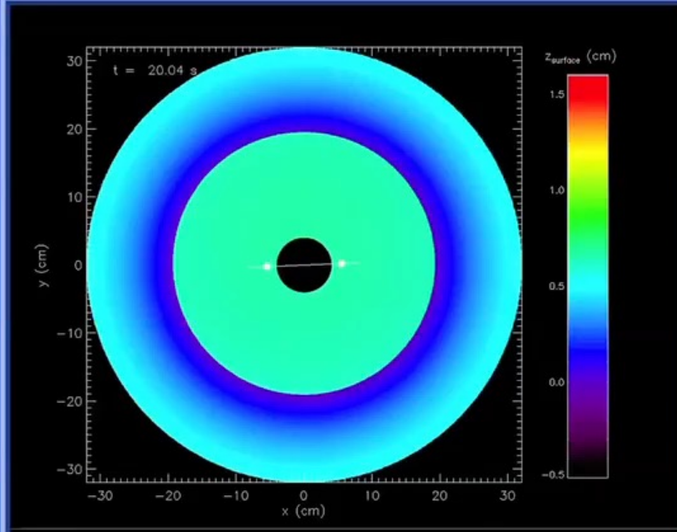

Simulation numérique de l'expérience hydraulique

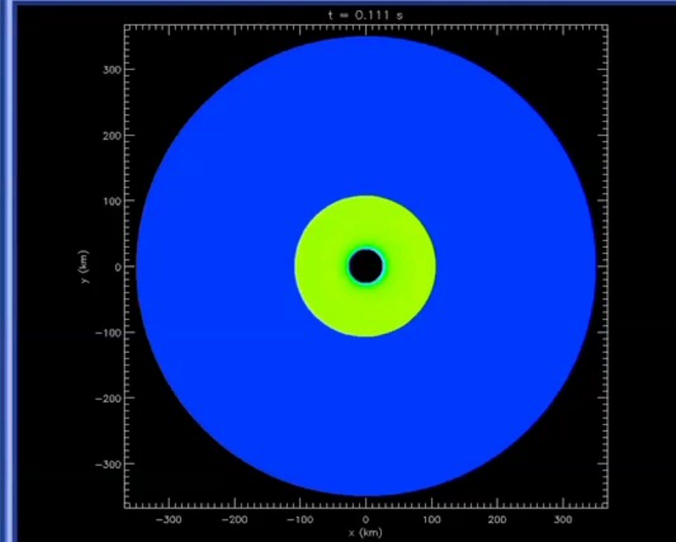

Simulation numérique de l'onde de choc dans le coeur de la supernova

SASI dynamics seems to be adiabatic

redistribution of angular momentum

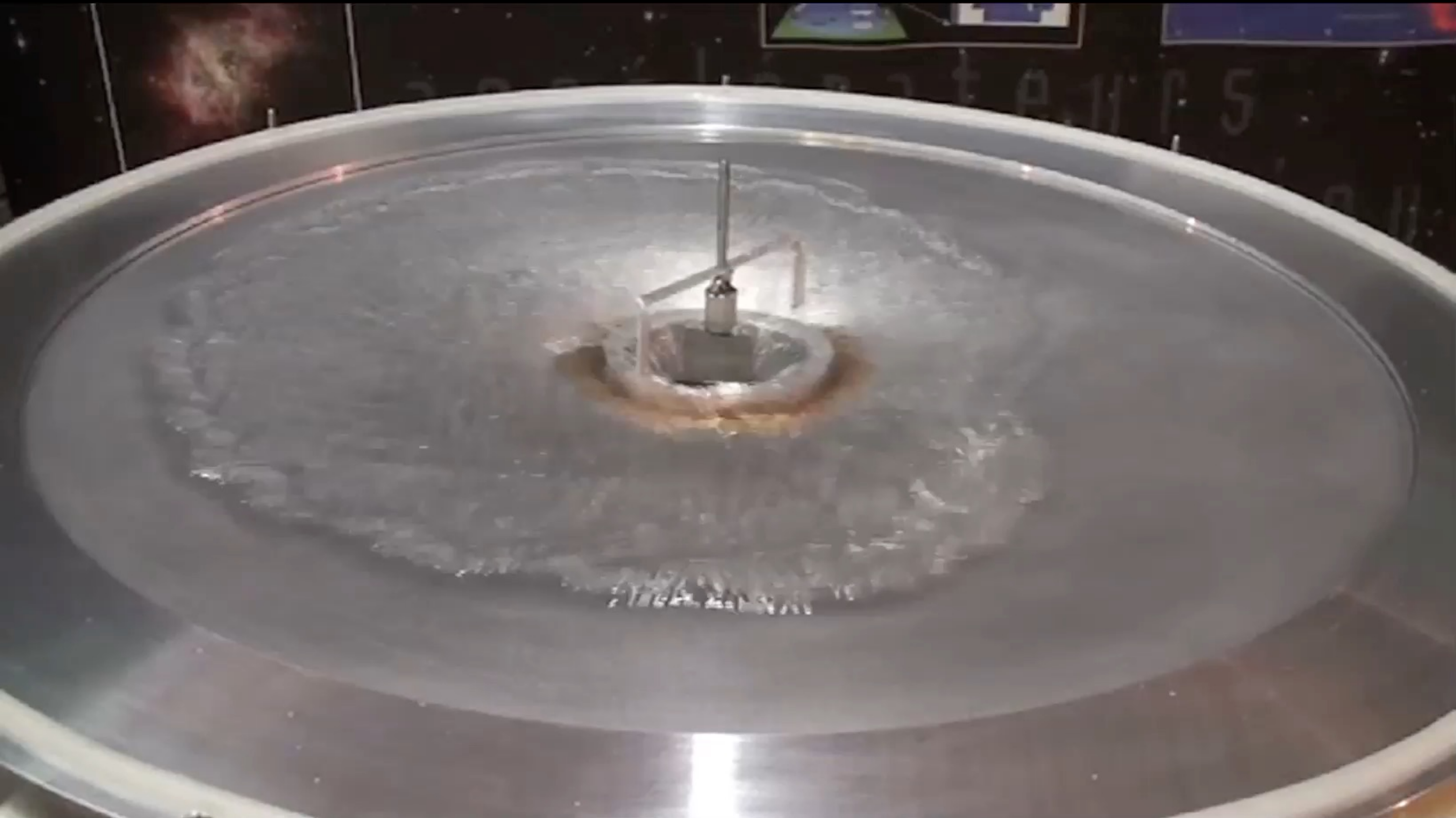

Shallow water analogy

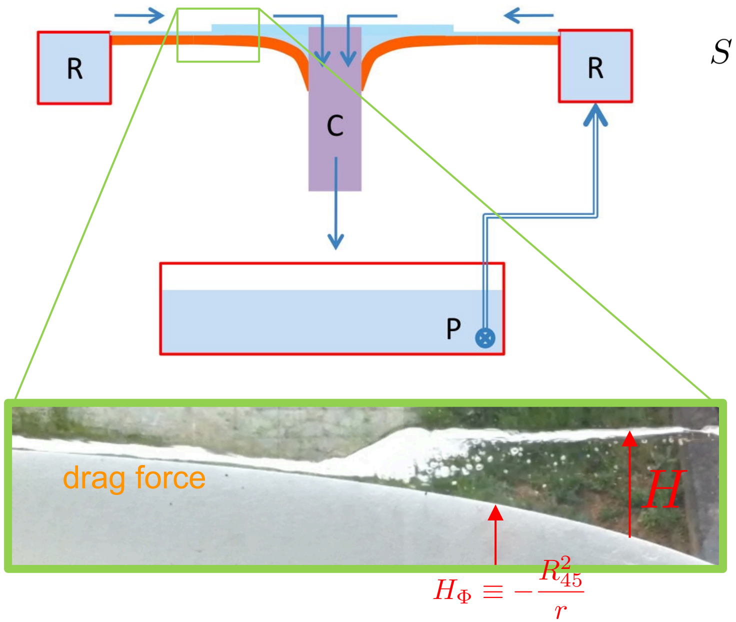

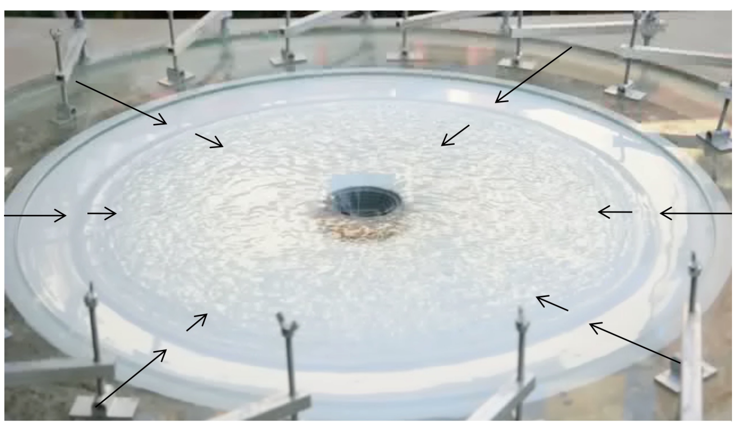

adiabatic gas

$$S \equiv \frac{1}{\gamma-1}\log\frac{p}{\rho^\gamma}$$

$$c_s^2 \equiv \frac{\gamma P}{\rho}$$

$$\Phi \equiv -\frac{GM_{ns}}{r}$$

$$\frac{\partial\rho}{\partial t} + \nabla\cdot(\rho v) = 0$$

$$\frac{\partial v}{\partial t} + (\nabla\times v)\times v + \nabla\left(\frac{v^2}{2} + \frac{c_s^2}{\gamma-1} + \Phi\right) = \frac{c_s^2}{\gamma}\nabla S$$

Inviscid shallow water is analogue to a homentropic gas γ=2

St Venant

$$c_{sw}^2 \equiv gH$$

$$\Phi \equiv gH_\Phi$$

$$\frac{\partial H}{\partial t} + \nabla\cdot(Hv) = 0$$

$$\frac{\partial v}{\partial t} + (\nabla\times v)\times v + \nabla\left(\frac{v^2}{2} + c_{sw}^2 + \Phi\right) = 0$$

(+drag force) $-3\nu\frac{v}{H^2}$

acoustic waves	↔	surface waves
shock wave		hydraulic jump
density ρ		depth H

expected scaling $$\frac{t_{ff}^{sh}}{t_{ff}^{jp}} \equiv \left(\frac{r_{sh}}{r_{jp}}\right)\left(\frac{r_{sh}gH_\Phi^{jp}}{GM_{ns}}\right)^{\frac{1}{2}} \sim 10^{-2}$$

shock radius $\times 10^{-6}$ 200 km → 20 cm

oscillation period $\times 10^{2}$ 30 ms → 3 s

adiabatic inner boundary condition inspired by the shallow water experiment

Stellar SASI:

- spherical geometry
- $\gamma=4/3$
- buoyancy effects
- neutronization at the NS surface

non adiabatic cooling/heating $\mathcal{L} = A_{\rm cool}\rho^{\beta-\alpha}p^{\alpha}$ (ν-processes)

➢ 4th order differential system

$$\delta h \equiv \frac{\delta v_r}{v_r} + \frac{\delta\rho}{\rho}$$

$$\delta K \equiv -imrv_r\delta w + m^2\frac{c^2}{\gamma}\delta S$$

baroclinic production of z-vorticity δw

$$L \equiv rv_\phi = r^2\Omega$$

$$\boxed{\omega' \equiv \omega - \frac{mL}{r^2}}$$

$$\left\{\begin{array}{rcl}
\frac{\partial}{\partial r}(r\delta v_\phi) &=& \frac{im}{v_r}\left(v_r\delta v_r - \frac{\delta K}{m^2} + \frac{c^2}{\gamma}\delta S\right)\\
\frac{\partial\delta h}{\partial r} &=& \frac{i\omega'}{v_r}\frac{\delta\rho}{\rho} - \frac{im}{rv_r}\delta v_\phi\ ,\\
\left(\frac{\partial}{\partial r} - \frac{i\omega'}{v_r}\right)\delta S &=& \delta\left(\frac{\mathcal{L}}{pv_r}\right)\ ,\\
\left(\frac{\partial}{\partial r} - \frac{i\omega'}{v_r}\right)\frac{\delta K}{m^2} &=& \delta\left(\frac{\mathcal{L}}{\rho v_r}\right)\ .
\end{array}\right.$$

Yamasaki & Foglizzo 08

Shallow water analogue:

- cylindrical geometry
- $\gamma=2$
- homentropic fluid
- adiabatic inner boundary

adiabatic evolution

➢ linear conservation of $rv_r\delta w$

➢ 2nd order differential system

➢ acoustic oscillator forced by the advection of vorticity

$$\mathrm{d}X \equiv \frac{v_r}{1-\mathcal{M}^2}\mathrm{d}r,$$

$$Y \equiv r\delta v_\phi \mathrm{e}^{\int_{\rm sh}\frac{i\omega'\mathcal{M}^2}{1-\mathcal{M}^2}\frac{\mathrm{d}r}{v_r}},$$

$$\left\{\begin{array}{l}
\frac{\partial^2 Y}{\partial X^2} + \left[\frac{\omega'^2}{c^2} - \frac{m^2}{r^2}(1-\mathcal{M}^2)\right]\frac{Y}{v_r^2} = \mathcal{S},\\
\mathcal{S} \equiv -(rv_r\delta w)_{\rm sh}\mathrm{e}^{\int_{\rm sh}\frac{i\omega'}{c^2}\mathrm{d}X}\frac{\partial}{\partial X}\left(\frac{\mathrm{e}^{\int_{\rm sh}\frac{i\omega'}{v_r}\mathrm{d}r}}{v^2}\right)
\end{array}\right.$$

Boundary conditions at the shock

The shock surface is perturbed with a radial displacement and velocity $\Delta v \equiv -i\omega\Delta\zeta$

In the direction **n** normal to the perturbed shock, conservation of the

-mass flux $[(H+\delta H)(v+\delta v-\Delta v)_\perp]_{r_{\rm sh}+\Delta\zeta}=0$

-momentum flux $\left[\frac{g}{2}(H+\delta H)^2+(H+\delta H)(v+\delta v-\Delta v)_\perp^2\right]_{r_{\rm sh}+\Delta\zeta}=0$

-energy flux : not conserved across the shock

In the tangential direction, conservation of the

-transverse momentum flux $\left[(H+\delta H)(v+\delta v-\Delta v)_\parallel(v+\delta v-\Delta v)_\perp\right]_{r_{\rm sh}+\Delta\zeta}=0$

$$\mathrm{Fr}\equiv\frac{v}{(gH)^{\frac{1}{2}}}$$

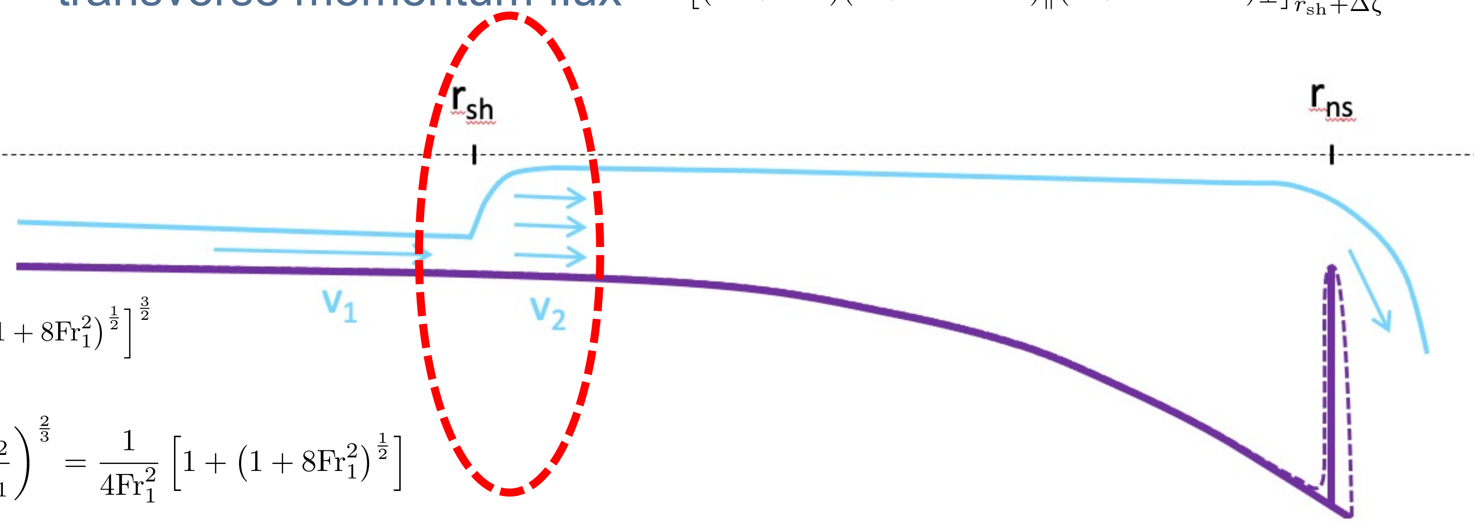

$$\mathrm{Fr}_2=\frac{1}{8\mathrm{Fr}_1^2}\left[1+(1+8\mathrm{Fr}_1^2)^{\frac{1}{2}}\right]^{\frac{3}{2}}$$

$$\frac{v_2}{v_1}=\frac{H_1}{H_2}=\left(\frac{\mathrm{Fr}_2}{\mathrm{Fr}_1}\right)^{\frac{2}{3}}=\frac{1}{4\mathrm{Fr}_1^2}\left[1+(1+8\mathrm{Fr}_1^2)^{\frac{1}{2}}\right]$$

Inner boundary condition

option 1 : δv_r=0 at the hard surface of the neutron star (Walk+23)

option 2: outgoing acoustic wave and outgoing vorticity perturbations (F+06, F09)

option 3: critical point mimicking the experiment (F+12)

-set by the regularity of the radial gradient of perturbed quantities

-can be generalized for a gas in 3D to build an adiabatic model

$$2\pi r_{\rm ns} H_{\rm edge} |v_{\rm ns}| = Q,$$
$$v_{\rm ns}^2 = g H_{\rm edge}.$$

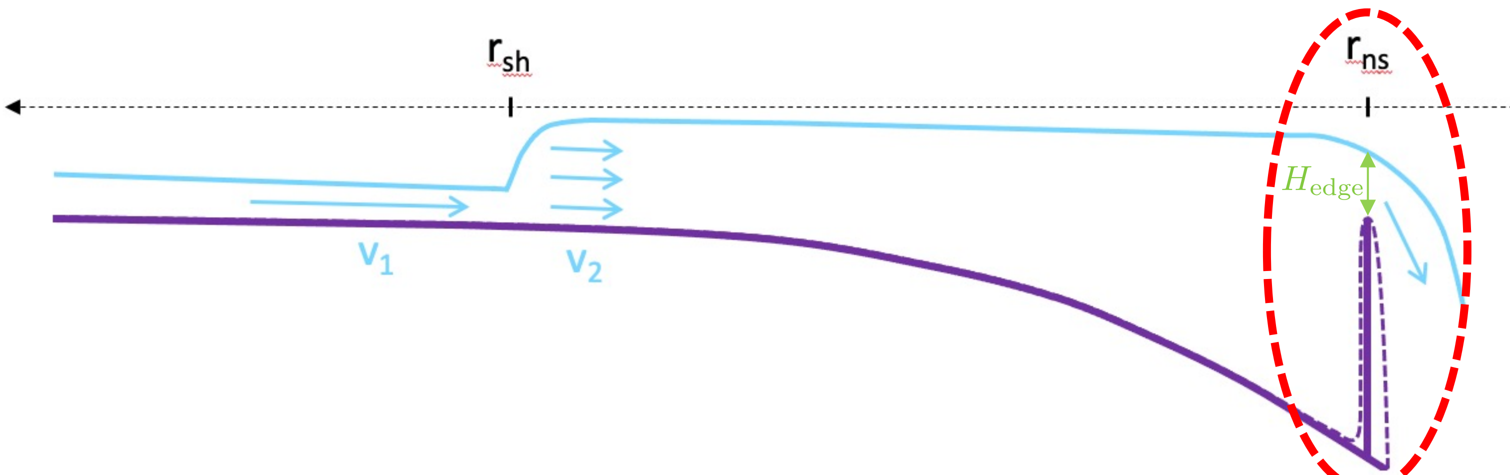

Shallow water model of the experiment including a viscous drag

$$c^2 \equiv gH,$$
$$\Phi \equiv gH_\Phi,$$
$$H_\Phi \equiv -\frac{(5.6\mathrm{cm})^2}{r}.$$

$$\frac{\partial H}{\partial t} + \nabla\cdot(Hv) = 0$$

$$\frac{\partial v}{\partial t} + (\nabla\times v)\times v + \nabla\left[\frac{v^2}{2} + c^2 + \Phi\right] = -\alpha\nu_{\mathrm{w}}\frac{v}{H^2}$$

perturbative analysis

$$\delta f \equiv v_r\delta v_r + g\delta H,$$
$$\delta h \equiv \frac{\delta v_r}{v_r} + \frac{\delta H}{H}.$$

$$\frac{\mathrm{d}\delta f}{\mathrm{d}r} = \frac{i\omega v_r}{1-\mathrm{Fr}^2}\left(\delta h - \frac{\delta f}{c^2}\right) + \frac{\bar{\nu}v_r}{H^2(1-\mathrm{Fr}^2)}\left[3\frac{\delta f}{c^2} - (1+2\mathrm{Fr}^2)\delta h\right], \qquad (7)$$

$$\frac{\mathrm{d}\delta h}{\mathrm{d}r} = \frac{i\omega}{v_r(1-\mathrm{Fr}^2)}\left(\frac{\delta f}{c^2} - \mathrm{Fr}^2\delta h\right) - \frac{im}{r^2 v_r}r\delta v_\theta, \qquad (8)$$

$$\frac{\mathrm{d}r\delta v_\theta}{\mathrm{d}r} = \frac{imv_r}{1-\mathrm{Fr}^2}\left(\delta h - \frac{\delta f}{v_r^2}\right) + \left(\frac{i\omega}{v_r} - \frac{\bar{\nu}}{v_r H^2}\right)r\delta v_\theta (9)$$

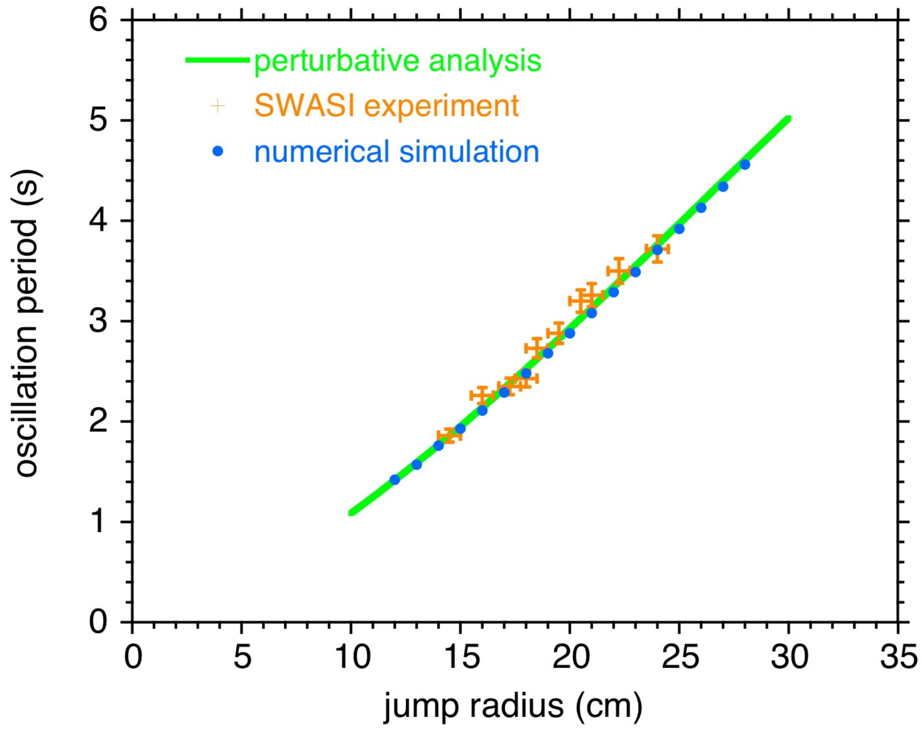

inner boundary condition:
regularity of the critical point

$$\delta f_* = c_{\mathrm{s}}^2\delta h_*,$$
$$c_s^2 \equiv \left(\frac{Qg}{2\pi R_*}\right)^{\frac{2}{3}}.$$

Foglizzo, Masset, Guilet, Durand
PRL (2012)

Comparison of the experiment with the St Venant model

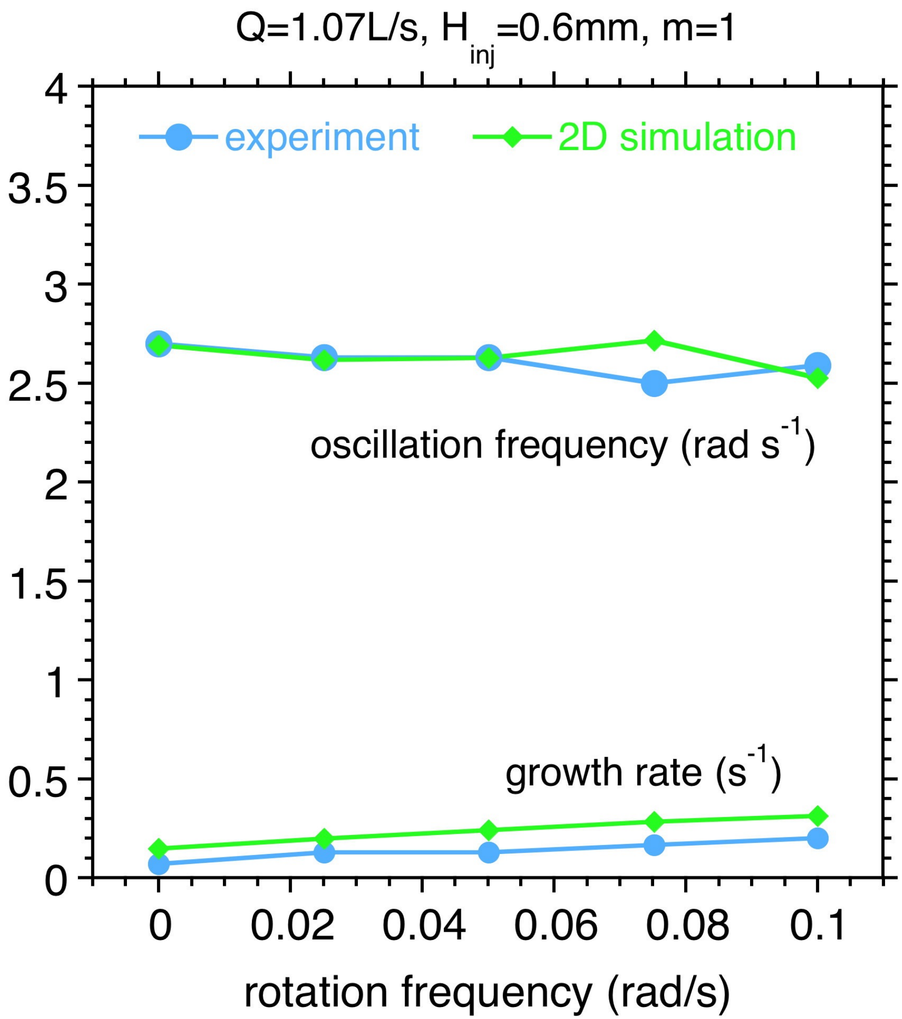

-surprisingly good frequency agreement, despite
- -2D shallow water modeling,
- -laminar drag without any free parameter,
- -ignoring turbulence,
- -ignoring surface tension,
- -ignoring the radial extension of the jump

-experimental growth rates are systematically lower by $\Delta\omega_i \sim 0.2\ s^{-1}$

Outline

Astrophysics background

Experiment and St Venant model
- Experimental setup
- Idealized St Venant model
- Comparing the model to the experiment

Physical understanding of linear processes
- Instability mechanism
- Slower growth in the experiment
- Destabilizing effect of rotation

Non linear challenges
- Saturation mechanism
- Impact of turbulence
- Surfing optimization

Benefits for astrophysics

Interaction of advected and acoustic perturbations

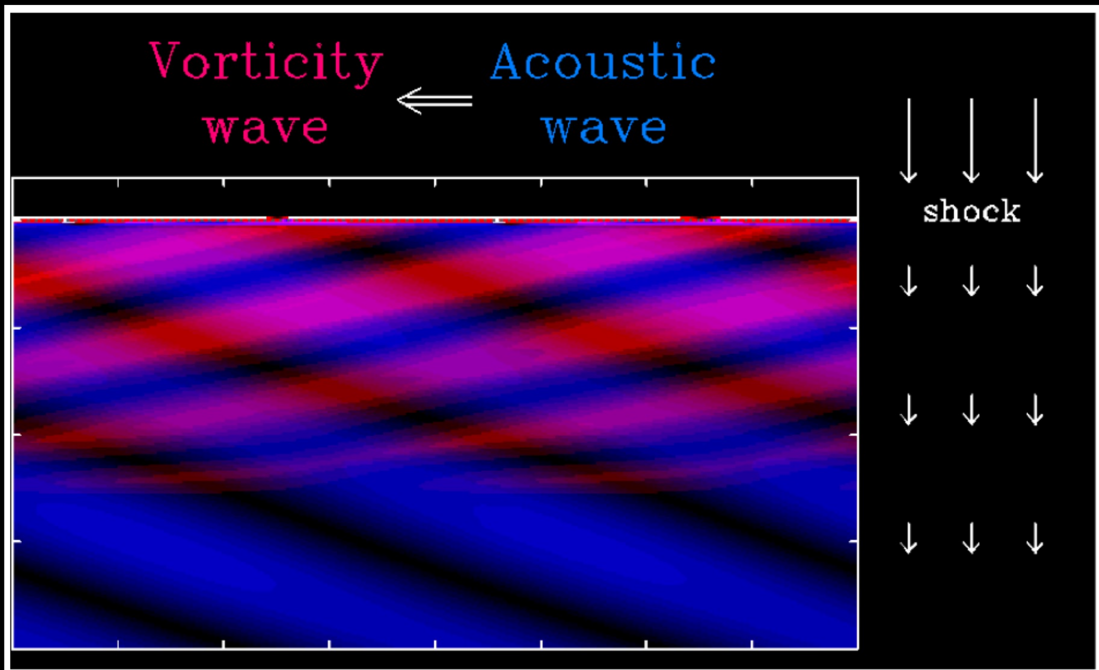

Sato+09

In a uniform stationary flow, advected and acoustic perturbations ignore each other linearly.

If the stationary flow involves gradients, these perturbations are linearly coupled

The advected perturbations are source terms in the acoustic equation

$$\frac{\partial^2 Y}{\partial X^2} + \left[\frac{\omega'^2}{c^2} - \frac{m^2}{r^2}(1-\mathcal{M}^2)\right]\frac{Y}{v_r^2} = \mathcal{S},$$

$$\mathcal{S} \equiv -(r v_r \delta w)_{\rm sh}\, e^{\int_{\rm sh} \frac{i\omega'}{c^2} {\rm d}X} \frac{\partial}{\partial X}\left(\frac{e^{\int_{\rm sh}\frac{i\omega'}{v_r}{\rm d}r}}{v^2}\right)$$

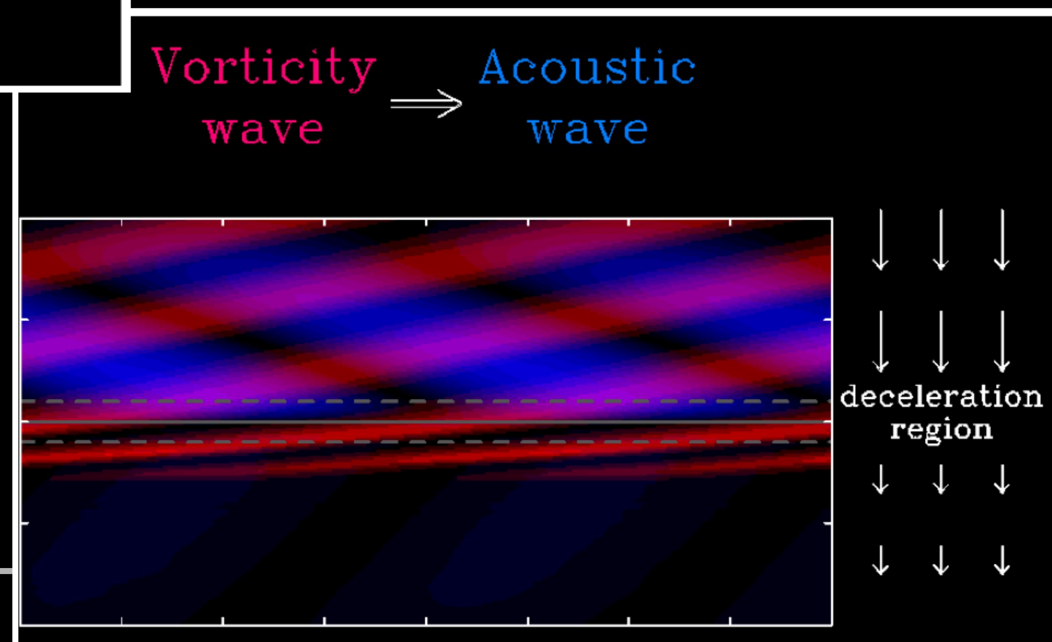

Interaction of advected and acoustic perturbations

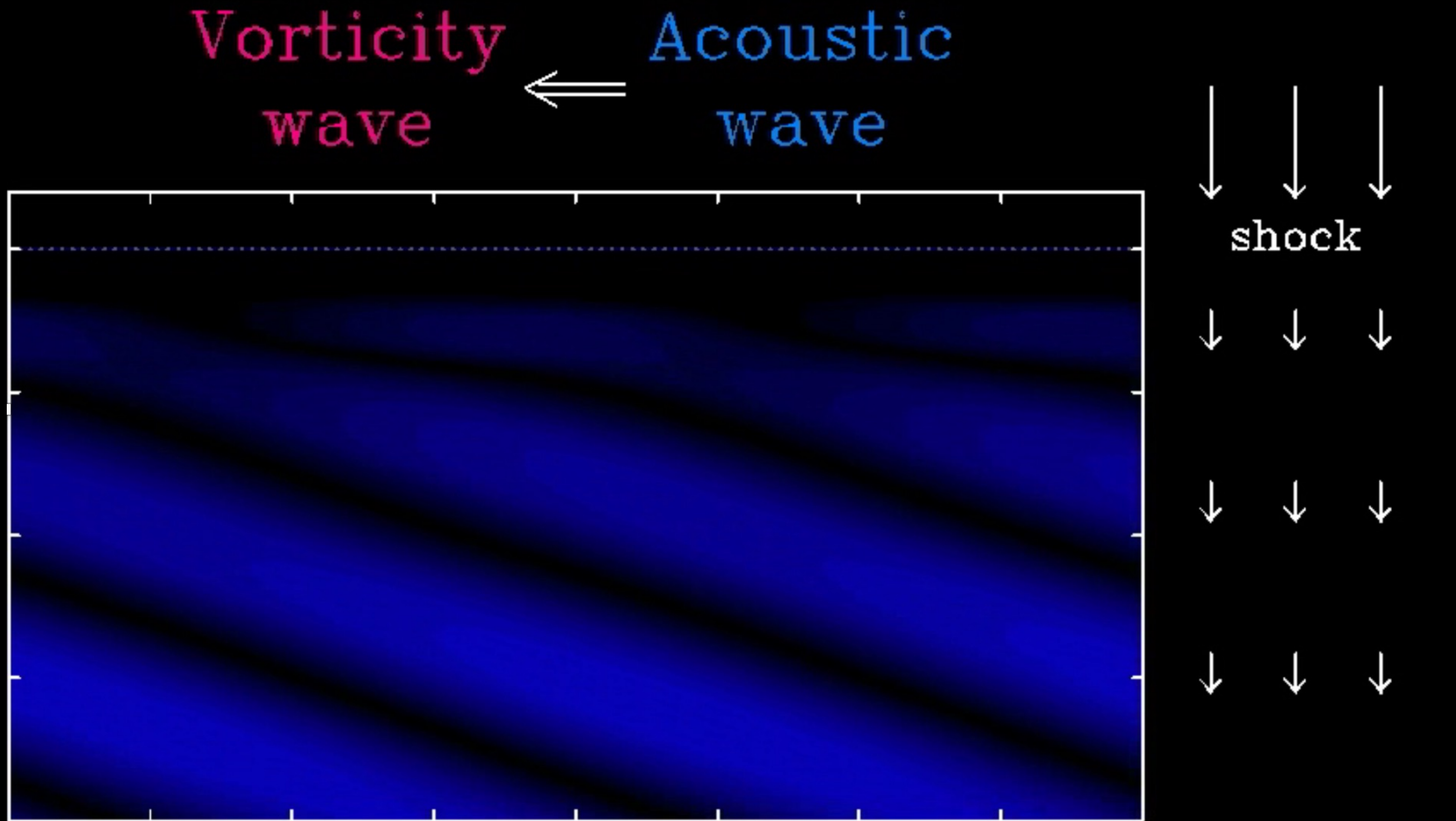

Shallow water analogue of the vortical-acoustic coupling

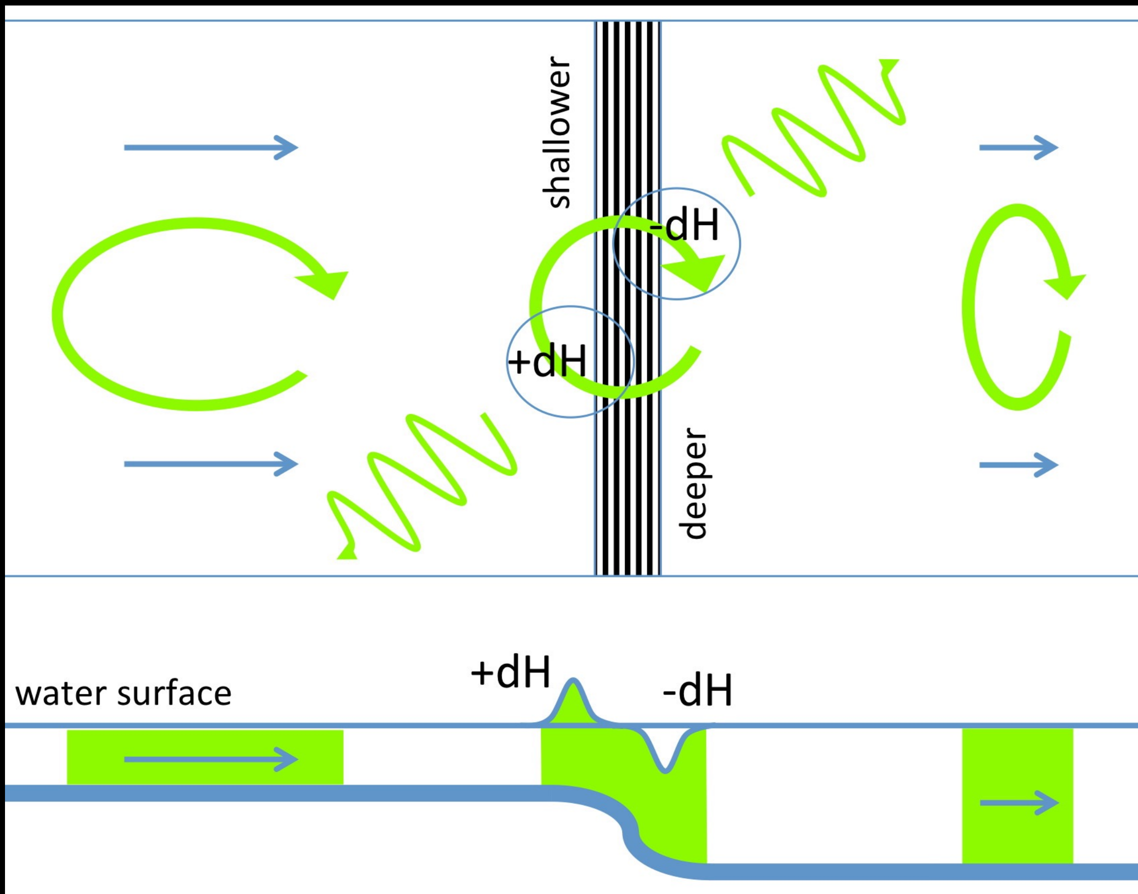

The vortical motion exchanges deep and shallow regions as the perturbation is advected over a change of depth

A planar toy model for the advective-acoustic coupling

The planar geometry and uniform flow between the shock and the compact deceleration region allows for a fully analytic calculation

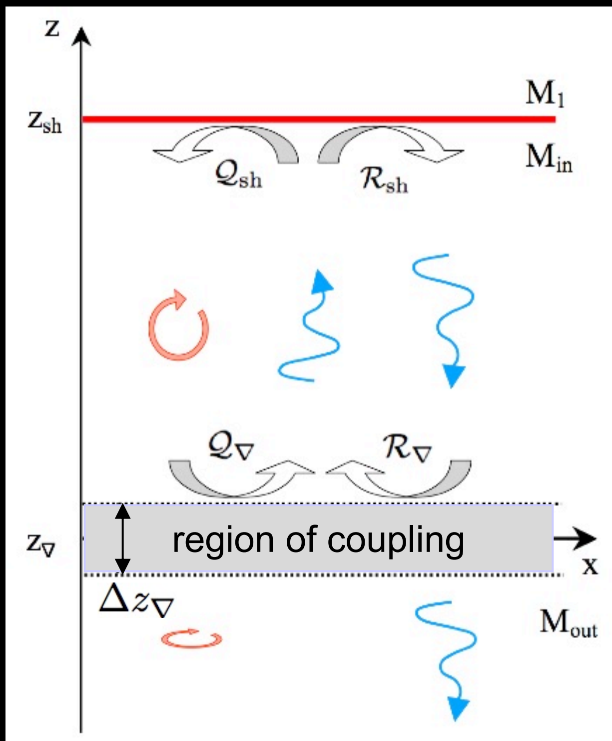

advective-acoustic cycle efficiency $\mathcal{Q} \equiv \mathcal{Q}_{sh}\mathcal{Q}_\nabla$

timescale $\tau_{\mathcal{Q}}$

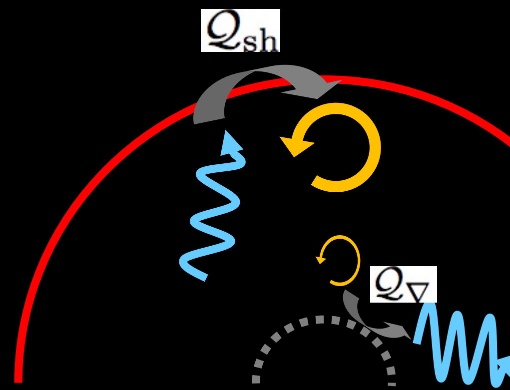

purely acoustic cycle efficiency $\mathcal{R} \equiv \mathcal{R}_{sh}\mathcal{R}_\nabla$

timescale $\tau_{\mathcal{R}}$

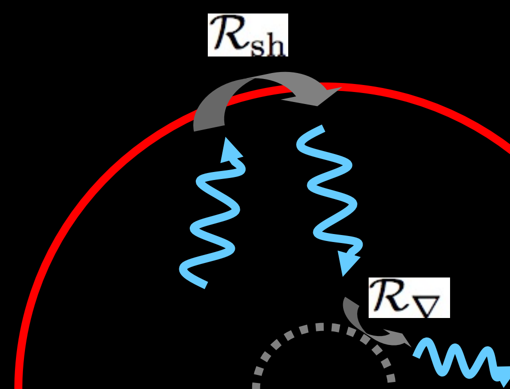

$$\mathcal{Q}e^{i\omega\tau_{\mathcal{Q}}} + \mathcal{R}e^{i\omega\tau_{\mathcal{R}}} = 1$$

Explicit analytical expressions for the coupling efficiencies for $\Delta z_\nabla \ll |z_{sh} - z_\nabla|$

A set of complex eigenfrequencies ω satisfy the phase equation relating the two cycles

$$\mathcal{Q}e^{i\omega\tau_{\mathcal{Q}}} + \mathcal{R}e^{i\omega\tau_{\mathcal{R}}} = 1$$

The coupling effciencies are defined from the ratio of energy densities δf^-, δf^+, δf_{adv} associated to acoustic and advected perturbations

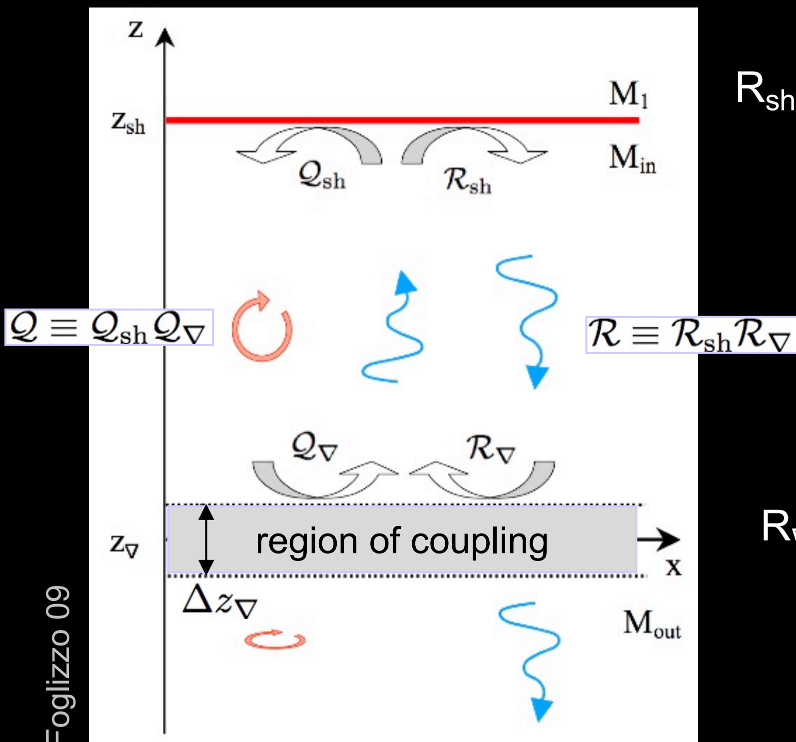

Foglizzo 09

R_{sh}, Q_{sh} are deduced from the conservation of mass, momentum and energy fluxes across a perturbed shock

$$\mathcal{R}_{sh} \equiv \frac{\delta f_{sh}^+}{\delta f_{sh}^-} = \frac{1+\mu_{sh}\mathcal{M}_{sh}}{1-\mu_{sh}\mathcal{M}_{sh}}\frac{\delta p_{sh}^+}{\delta p_{sh}^-},$$
$$= -\frac{\mu_{sh}^2 - 2\mathcal{M}_{sh}\mu_{sh} + \mathcal{M}_1^{-2}}{\mu_{sh}^2 + 2\mathcal{M}_{sh}\mu_{sh} + \mathcal{M}_1^{-2}}\frac{1+\mu_{sh}\mathcal{M}_{sh}}{1-\mu_{sh}\mathcal{M}_{sh}}.$$

$$\mathcal{Q}_{sh} \equiv \frac{\delta f_{sh}^S}{\delta f_{sh}^-} = \frac{1}{1-\mu_{sh}\mathcal{M}_{sh}}\frac{p_{sh}\delta S_{sh}}{\delta p_{sh}^-},$$
$$= \frac{2}{\mathcal{M}_{sh}}\frac{1-\mathcal{M}_{sh}^2}{1+\gamma\mathcal{M}_{sh}^2}\left(1-\frac{\mathcal{M}_{sh}^2}{\mathcal{M}_1^2}\right)$$
$$\times\frac{\mu_{sh}}{(1-\mu_{sh}\mathcal{M}_{sh})(\mu_{sh}^2+2\mu_{sh}\mathcal{M}_{sh}+\mathcal{M}_1^{-2})},$$

$$\mu^2 \equiv 1 - \frac{k_x^2c^2}{\omega^2}(1-\mathcal{M}^2)$$

R_∇, Q_∇ are deduced from the conservation of mass and energy fluxes across the compact deceleration region

$$\mathcal{R}_\nabla = \frac{\mu_{in}\mathcal{M}_{out}c_{out}^2 - \mu_{out}\mathcal{M}_{in}c_{in}^2}{\mu_{in}\mathcal{M}_{out}c_{out}^2 + \mu_{out}\mathcal{M}_{in}c_{in}^2}e^{i\omega\tau_{\mathcal{R}}},$$

$$\mathcal{Q}_\nabla = \frac{\mathcal{M}_{out}+\mu_{out}}{1+\mu_{out}\mathcal{M}_{out}}\frac{e^{i\omega\tau_{\mathcal{Q}}}}{\mu_{out}\frac{c_{in}^2}{c_{out}^2}+\mu_{in}\frac{\mathcal{M}_{out}}{\mathcal{M}_{in}}}$$
$$\times\left[1-\frac{c_{in}^2}{c_{out}^2}+\frac{k_x^2c_{in}^2}{\omega^2}(\mathcal{M}_{in}^2-\mathcal{M}_{out}^2)\right],$$

Interferences between the advective-acoustic cycle and the purely acoustic cycle

$$Qe^{i\omega\tau_Q} + \mathcal{R}e^{i\omega\tau_\mathcal{R}} = 1$$

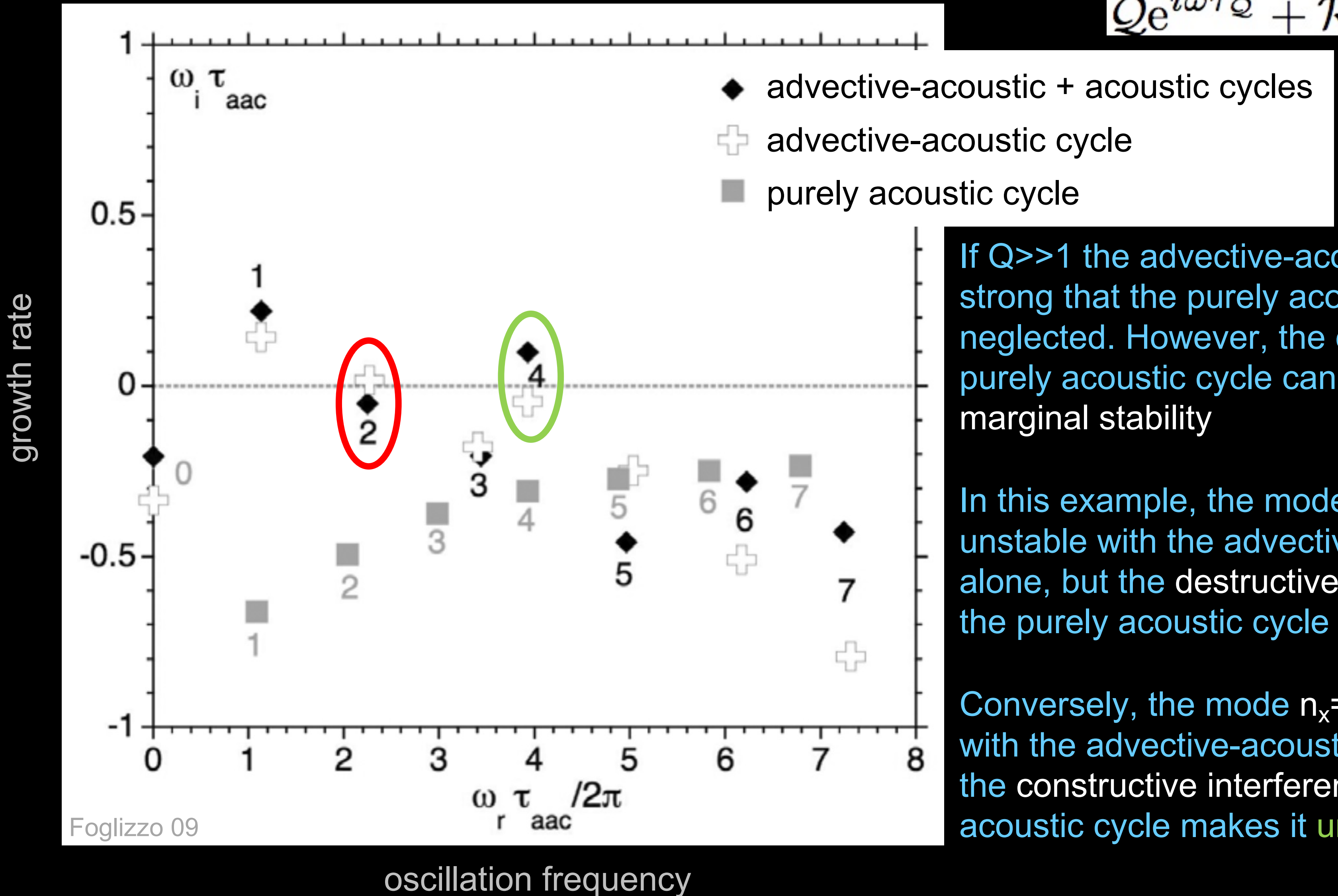

If Q>>1 the advective-acoustic cyle is so strong that the purely acoustic cycle can be neglected. However, the contribution of the purely acoustic cycle can be decisive near marginal stability

In this example, the mode n_x=2 would be unstable with the advective-acoustic cycle alone, but the destructive interference with the purely acoustic cycle makes it stable

Conversely, the mode n_x=4 would be stable with the advective-acoustic cycle alone, but the constructive interference with the purely acoustic cycle makes it unstable

see also Fernandez & Thompson 09

Understanding the efficiency of the acoustic feedback (Foglizzo 09)

$M_1=5$, $\gamma=4/3$, $T_{in}/T_{out}=0.75$

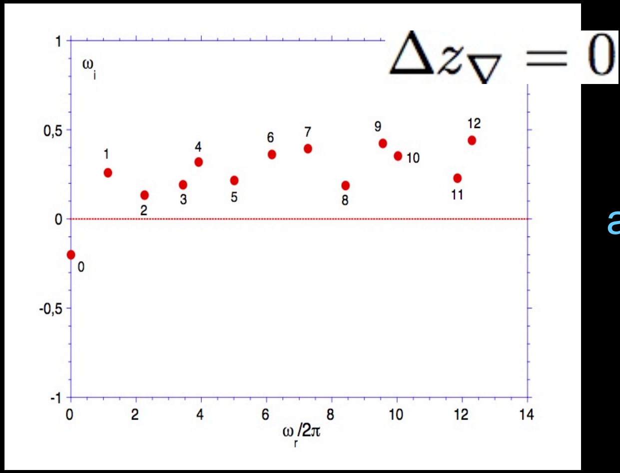

fully analytic

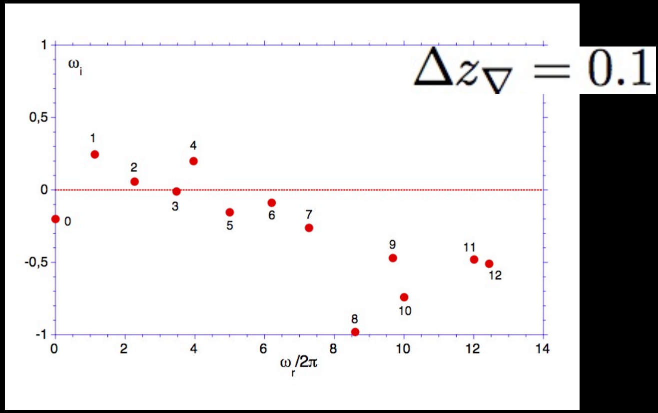

oscillation frequency

The finite lengthscale of the deceleration region introduces a frequency cut-off ω_∇ associated to the crossing time τ_∇

$$\boxed{\omega_\nabla \sim \frac{1}{\tau_\nabla}}$$

$$\mathcal{Q}_\nabla = \int_{\rm bc}^{\rm sh} b_0 \frac{\delta p_0}{p} e^{\int_{\rm sh} \frac{i\omega}{v} dz} \frac{\partial b_\nabla}{\partial z} dz,$$

forced oscillator

$$b_0 \equiv \frac{1}{2}\left(1+\frac{k_x^2 v_{\rm sh}^2}{\omega^2}\right)\left(1-\mathcal{R}_\nabla-\frac{1+\mathcal{R}_\nabla}{\mu_{\rm sh}\mathcal{M}_{\rm sh}}\right) \times \frac{1-\mathcal{M}^2}{1-\mathcal{M}_{\rm sh}^2}\frac{\mathcal{M}_{\rm sh}^2}{\mathcal{M}^2}\left(\frac{\delta p_0}{p}\right)_{\rm sh}^{-1} e^{-\int_{\rm sh}\frac{i\omega}{c}\frac{2\mathcal{M}}{1-\mathcal{M}^2}dz},$$

$$b_\nabla \equiv \frac{i\omega}{c_{\rm sh}^2}\,\frac{i\omega - 2v\frac{\partial \log \mathcal{M}}{\partial z}}{k_x^2\mathcal{M}^2+\frac{\omega^2}{c^2}-v\mathcal{M}^2\frac{\partial}{\partial z}\frac{i\omega}{v^2}}.$$

-large horizontal wavenumber perturbations correspond to higher frequencies.
-high frequency perturbations are stabilized by phase mixing above the cut-off frequency

→ SASI is a low frequency instability dominated by l=1,2

Beyond the ST Venant approximation: phase mixing of dragged vorticity ?

$$\mathrm{Re}_H \equiv \frac{Hv}{\nu} = 796 \left(\frac{Q}{1\mathrm{L/s}}\right)\left(\frac{20\mathrm{cm}}{R_{\mathrm{jump}}}\right) = 2650 \left(\frac{Q}{1\mathrm{L/s}}\right)\left(\frac{6\mathrm{cm}}{R_{\mathrm{NS}}}\right)$$

$$\mathrm{Re}_L \equiv (R_{\mathrm{inj}} - R_{\mathrm{jump}})\frac{v_{\mathrm{inj}}}{\nu} = 10^5 \left(\frac{Q}{1\mathrm{L/s}}\right)\left(\frac{0.6\mathrm{mm}}{H_{\mathrm{inj}}}\right)$$

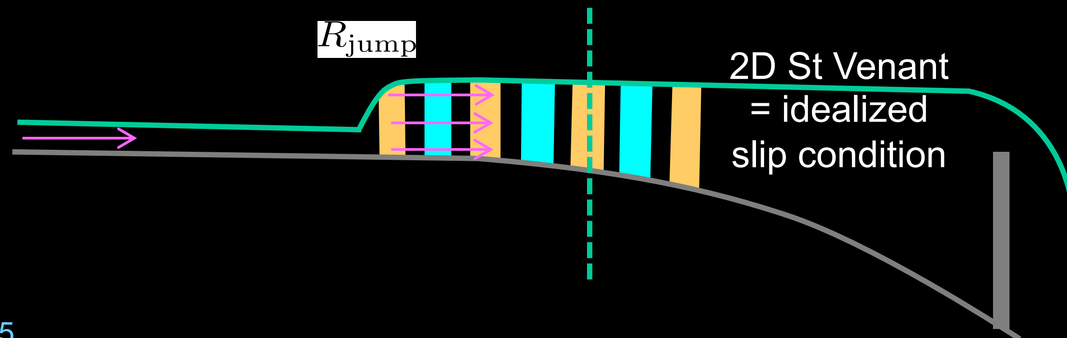

unknown vertical structure H(R)

- laminar/turbulent transition $\mathrm{Re}_L \sim 5\times10^5$
- vertical extension of the boundary layer
  - $\delta_{jp} \sim 2$mm if laminar ($4.91\ L/\mathrm{Re}_L^{1/2}$)
  - $\delta_{jp} \sim 5$mm if turbulent ($0.38\ L/\mathrm{Re}_L^{1/5}$)

$$\omega_{\mathrm{SASI}} \sim \frac{2\pi v_H}{\Delta R}$$

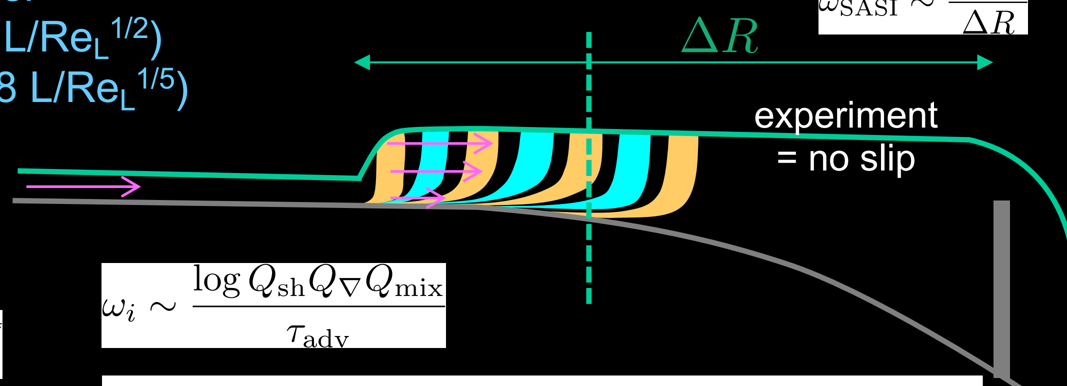

reference examples

- half-Poiseuille: $\frac{v(z)}{< v >} \sim \frac{3z}{2H}\left(2 - \frac{z}{H}\right)$
- turbulent prescription: $\frac{v(z)}{< v >} \sim \frac{8}{7}\left(\frac{z}{H}\right)^{\frac{1}{7}}$

$$\omega_i \sim \frac{\log Q_{\mathrm{sh}} Q_{\nabla} Q_{\mathrm{mix}}}{\tau_{\mathrm{adv}}}$$

The vertically averaged vorticity is damped by a factor Q_{mix}

$$Q_{\mathrm{mix}} \sim \int_0^H \frac{\mathrm{d}z}{H} \cos\left[\frac{\omega_{\mathrm{SASI}}\Delta R}{v(z)}\right] \sim 0.27\ (\mathrm{laminar}) \sim 0.52\ (\mathrm{turbulent})$$

order of magnitude estimate: $\Delta\omega_i \sim \frac{\log Q_{\mathrm{mix}}}{\tau_{\mathrm{adv}}}$

Comparison of the experiment with the shallow water equations

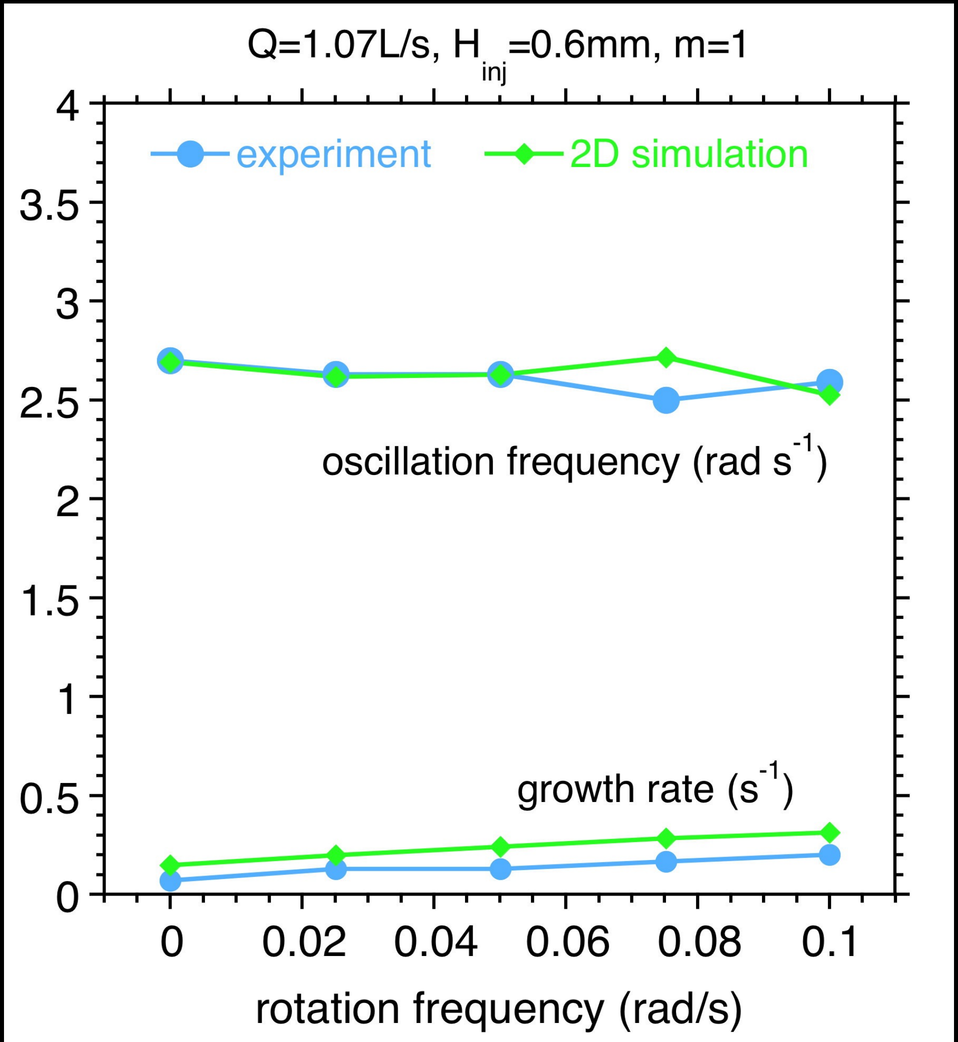

-surprisingly good frequency agreement, despite
- -2D shallow water modeling,
- -laminar drag without any free parameter,
- -ignoring turbulence,
- -ignoring surface tension,
- -ignoring the radial extension of the jump

-experimental growth rates are systematically lower by $\Delta\omega_i \sim 0.2\ s^{-1}$

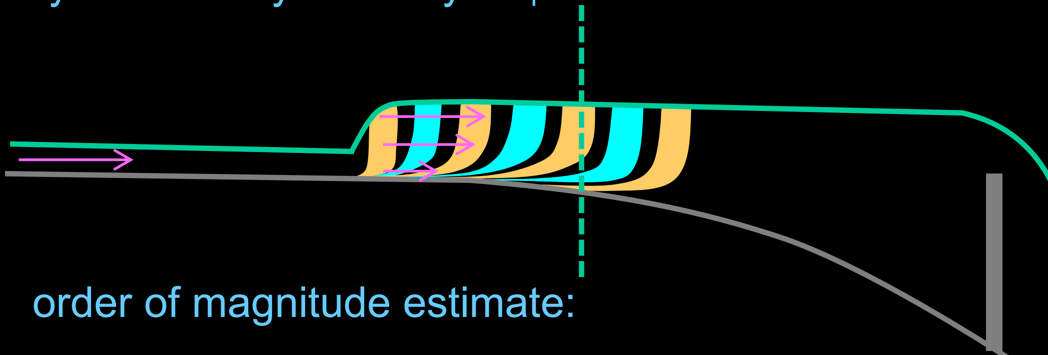

order of magnitude estimate:

$$\tau_{\rm adv} \sim \frac{2\pi}{\omega_r} \sim 2.4s$$

$$\frac{\log Q_{\rm mix}}{\tau_{\rm adv}} = -0.54s^{-1}(\text{laminar}) = -0.27s^{-1}(\text{turbulent})$$

Rotating progenitor: destabilization of the prograde mode

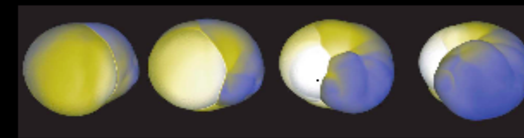

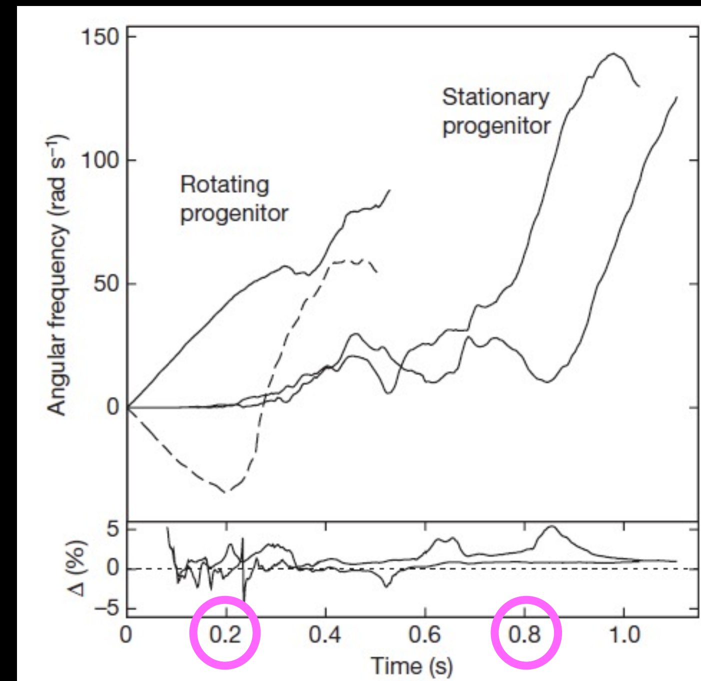

increased angular momentum in the post shock flow
+
decreased angular momentum in the neutron star
= 0

Blondin & Mezzacappa 07

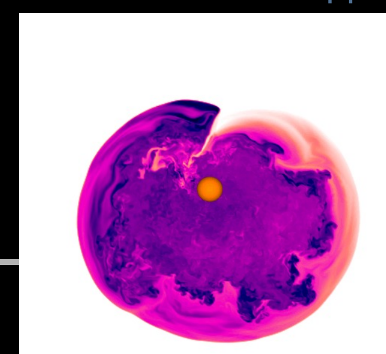

$$\boxed{\omega' \equiv \omega - \frac{mL}{r^2}}$$

the radial wavelength of the advected prograde vorticity perturbation is increased by differential rotation: de-mixing of the prograde mode

Outline

Astrophysics background

Experiment and St Venant model
- Experimental setup
- Idealized St Venant model
- Comparing the model to the experiment

Physical understanding of linear processes
- Instability mechanism
- Slower growth in the experiment
- Destabilizing effect of rotation

Non linear challenges
- Saturation mechanism
- Impact of turbulence
- Surfing optimization

Benefits for astrophysics

The saturation of SASI by parasitic instabilities

Guilet+10

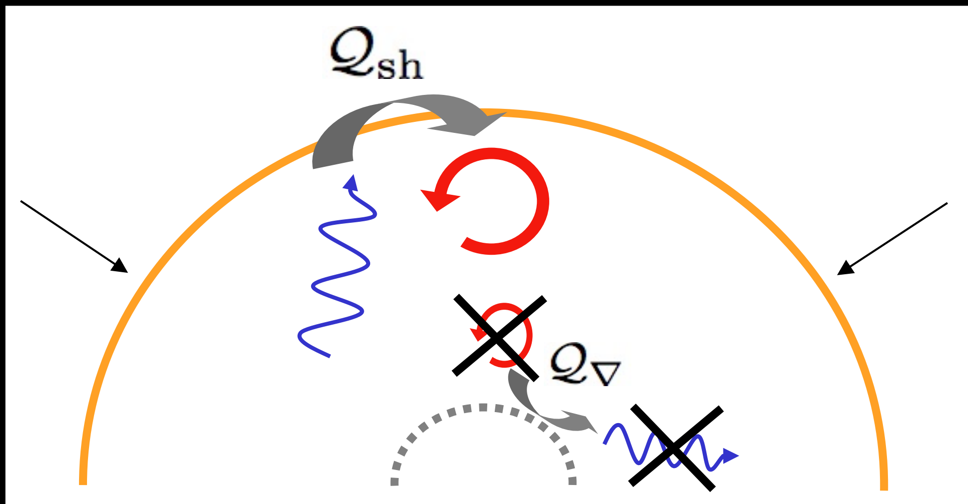

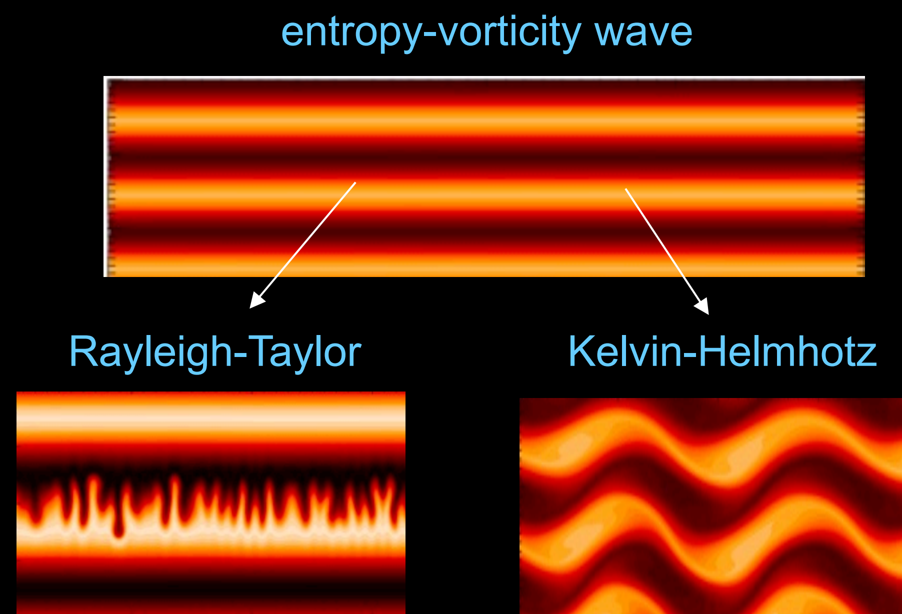

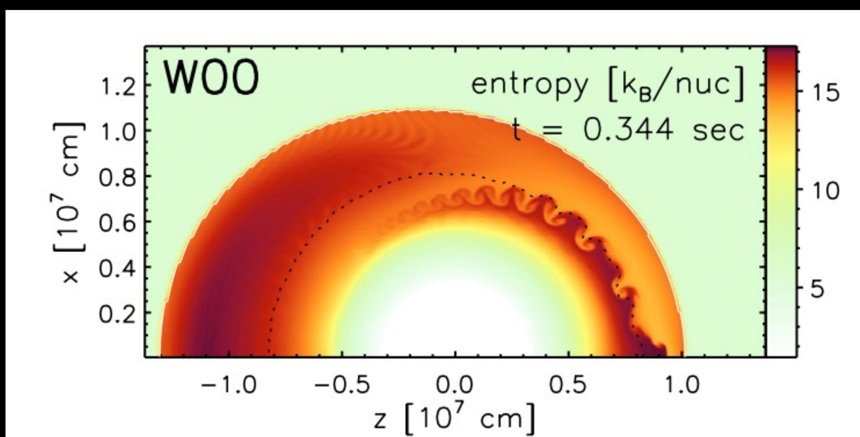

Entropy and vorticity waves produced by the shock oscillations are unstable to parasitic instabilities

Rayleigh-Taylor + Kelvin-Helmholtz

The advective-acoustic cycle is affected if

- the parasitic instabilities are able to propagate against the flow,
- their effective eulerian growth rate exceeds the SASI growth rate

Turbulent stabilization ?

$$H_\Phi \equiv -\frac{R_{45}^2}{r}$$

without rotation,
turbulent SASI @ 100L/s
seems less unstable than
laminar SASI @1L/s

$R_{45} = 5.6cm$

66cm

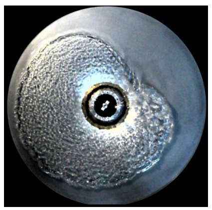

$$\lambda \equiv \frac{R'_{45}}{R_{45}} = 6.25$$

$$\mathrm{Re} \equiv \frac{hv}{\nu} = \mathrm{Fr}\frac{g^{\frac{1}{2}}h^{\frac{3}{2}}}{\nu}$$

$$6.25^{\frac{3}{2}} \sim 15.6$$

$$Q = 2\pi rvh = 2\pi\frac{r}{h}\mathrm{Fr}g^{\frac{1}{2}}h^{\frac{5}{2}}$$

$$6.25^{\frac{5}{2}} \sim 98$$

$$Q\frac{v^2}{2} = 2\pi rvh\frac{v^2}{2} = \pi\frac{r}{h}\mathrm{Fr}g^{\frac{3}{2}}h^{\frac{7}{2}}$$

$$6.25^{\frac{7}{2}} \sim 610$$

$R'_{45} = 35cm$

350cm

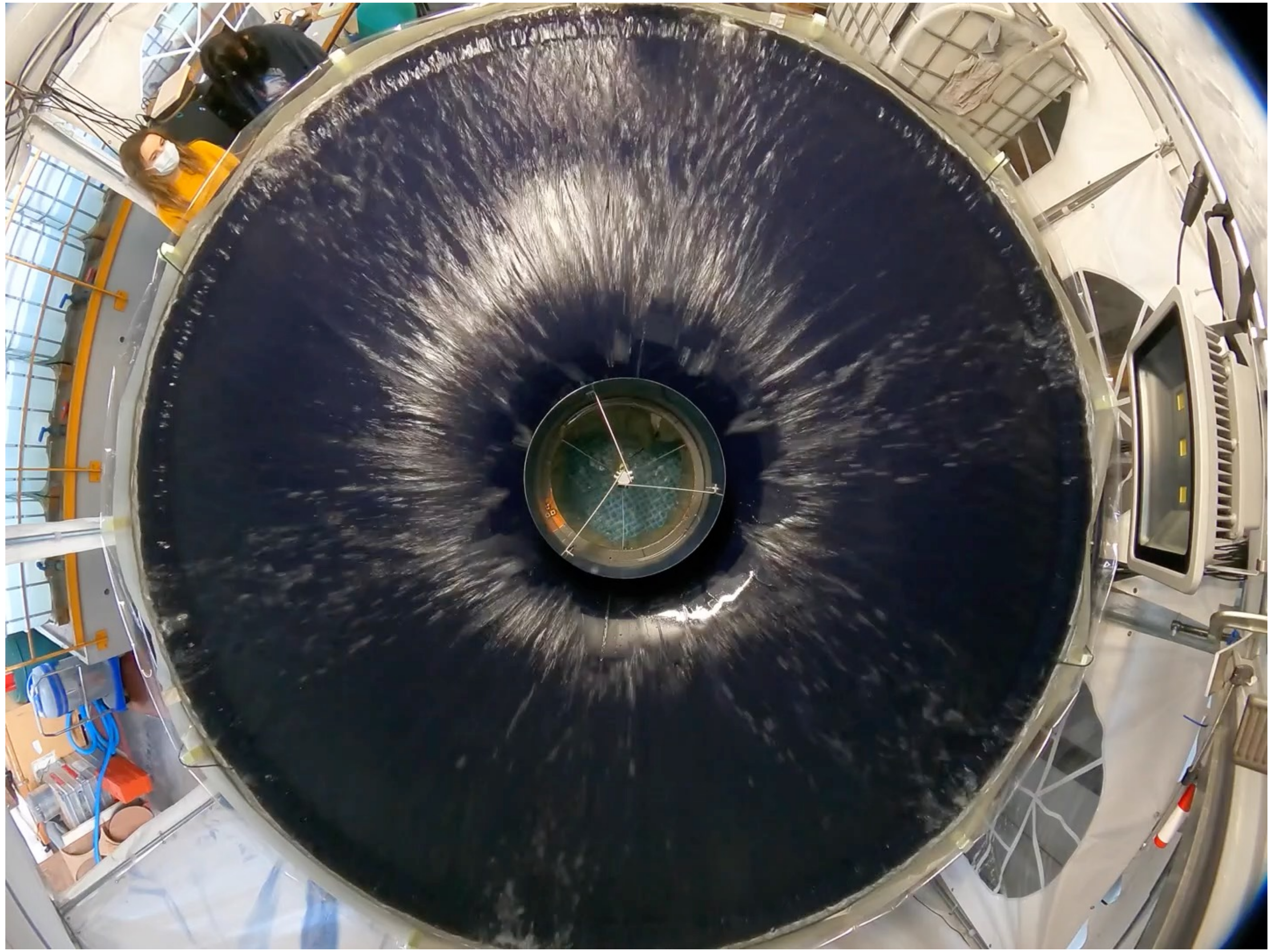

turbulent hydraulic jump

Saturated non linear evolution: towards a quasi stationary pattern?

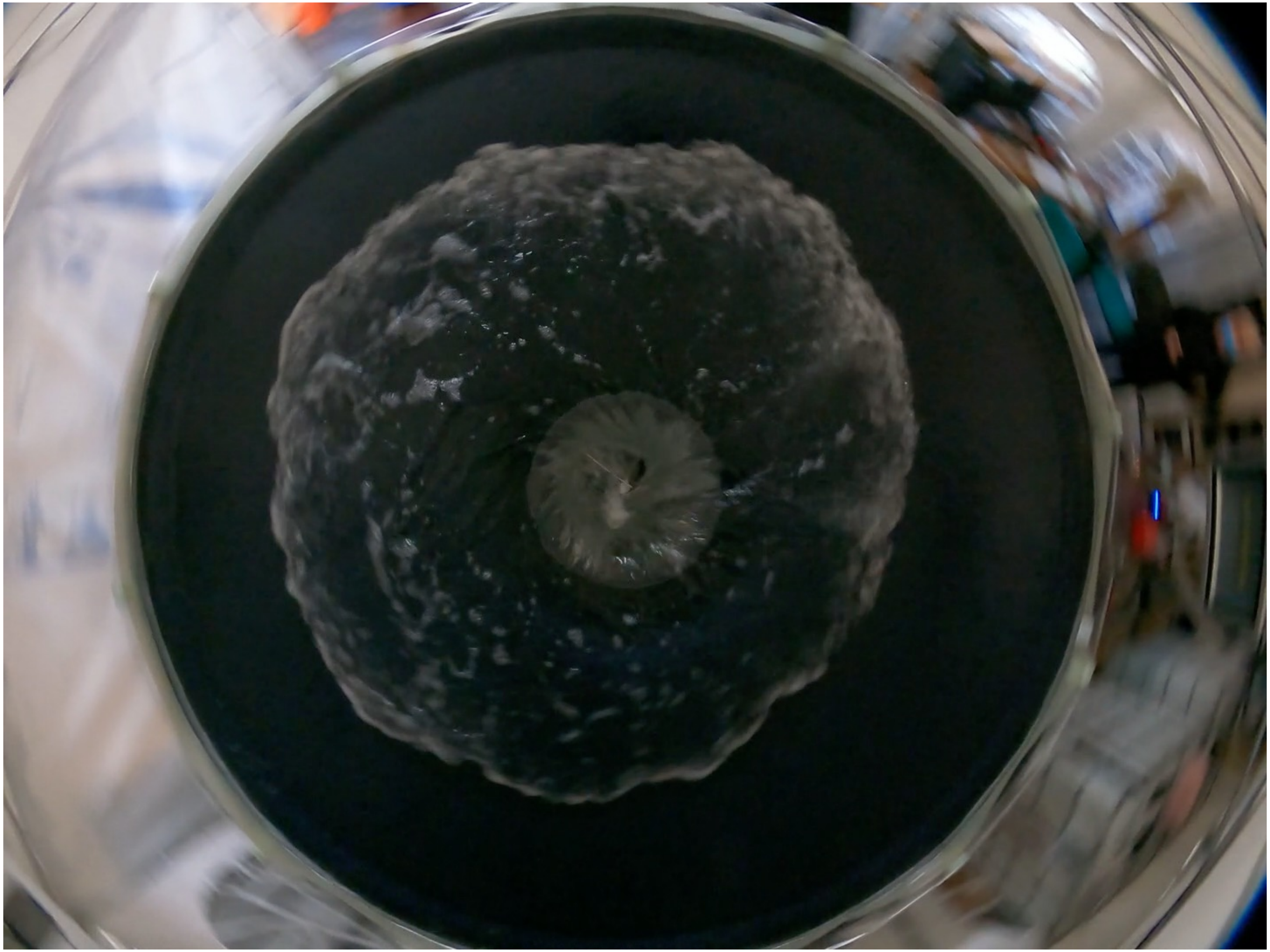

what is the asymptotic shape of the non linear saturated state?

Saturated non linear evolution: towards a quasi stationary pattern?

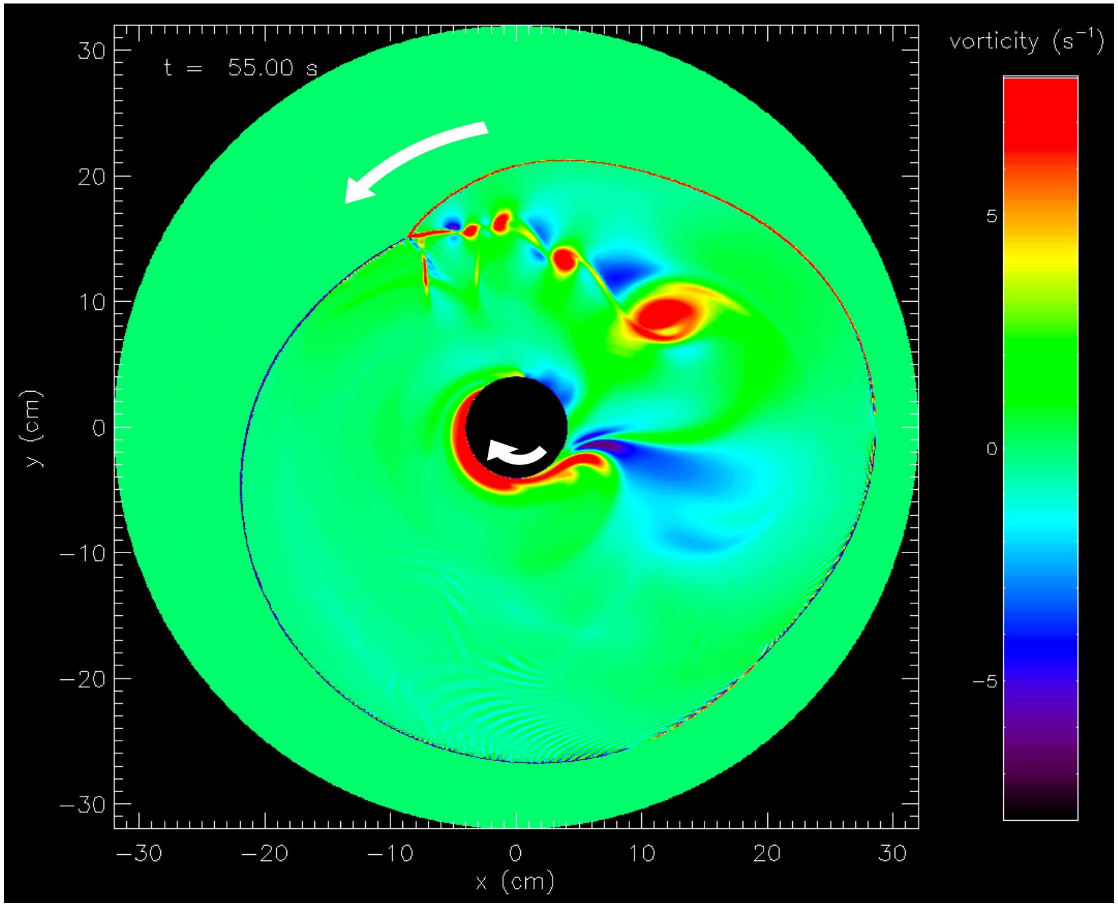

<u>triple point</u>:
fragmentation of the vorticity line
shedding discrete advected vortices:

-numerical convergence?

-no stationary asymptotic solution?

From supernova physics to circular wave surfing?

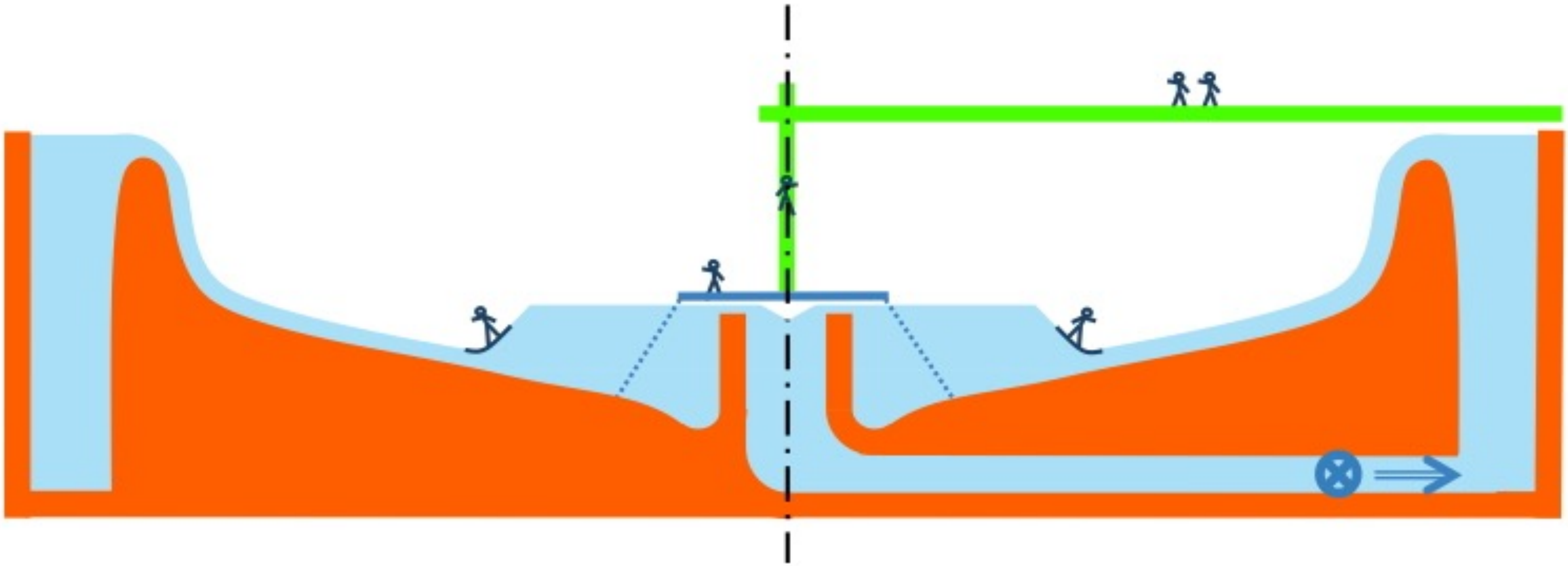

From supernova physics to circular wave surfing?

Outline

adiabatic gas flow
inspired by the shallow water experiment

Shallow water analogue:
- cylindrical geometry
- γ=2
- homentropic fluid
- adiabatic inner boundary

adiabatic evolution
- linear conservation of $rv_r\delta w$
- 2nd order differential system
- acoustic oscillator forced with source $\mathcal{S}$

$$\mathrm{dX} \equiv \frac{v_r}{1-\mathcal{M}^2}\mathrm{d}r,$$
$$Y \equiv r\delta v_\phi \mathrm{e}^{\int_{\mathrm{sh}} \frac{i\omega' \mathcal{M}^2}{1-\mathcal{M}^2}\frac{\mathrm{d}r}{v_r}},$$

$$\begin{cases} \dfrac{\partial^2 Y}{\partial X^2} + \left[\dfrac{\omega'^2}{c^2} - \dfrac{m^2}{r^2}(1-\mathcal{M}^2)\right]\dfrac{Y}{v_r^2} = \mathcal{S}, \\ \mathcal{S} \equiv -(rv_r\delta w)_{\mathrm{sh}}\mathrm{e}^{\int_{\mathrm{sh}}\frac{i\omega'}{c^2}\mathrm{d}X}\dfrac{\partial}{\partial X}\left(\dfrac{\mathrm{e}^{\int_{\mathrm{sh}}\frac{i\omega'}{v_r}\mathrm{d}r}}{v^2}\right) \end{cases}$$

Adiabatic extension:
- spherical geometry
- any γ
- buoyancy effects
- adiabatic inner boundary

adiabatic evolution
- linear conservation of δK + entropy δS
- 2nd order differential system
- acoustic oscillator forced with source $\mathcal{S}$

$$\delta K \equiv -imrv_r\delta w + m^2\frac{c^2}{\gamma}\delta S$$

$$\begin{cases} \dfrac{\partial^2 Y}{\partial X^2} + \left[\dfrac{\omega'^2}{c^2} - \dfrac{m^2}{r^2}(1-\mathcal{M}^2)\right]\dfrac{Y}{v_r^2} = \mathcal{S}, \\ \mathcal{S} \equiv -\dfrac{r_{\mathrm{sh}}}{v_{\mathrm{sh}}}\delta w_{\mathrm{sh}}\mathrm{e}^{\int_{\mathrm{sh}}\frac{i\omega'}{c^2}\mathrm{dX}}\dfrac{\partial}{\partial X}\left(\dfrac{\mathcal{M}_{\mathrm{sh}}^2}{\mathcal{M}^2}\mathrm{e}^{\int_{\mathrm{sh}}\frac{i\omega'}{v_r}\mathrm{d}r}\right) \end{cases}$$

Comparison of the non-adiabatic and adiabatic models

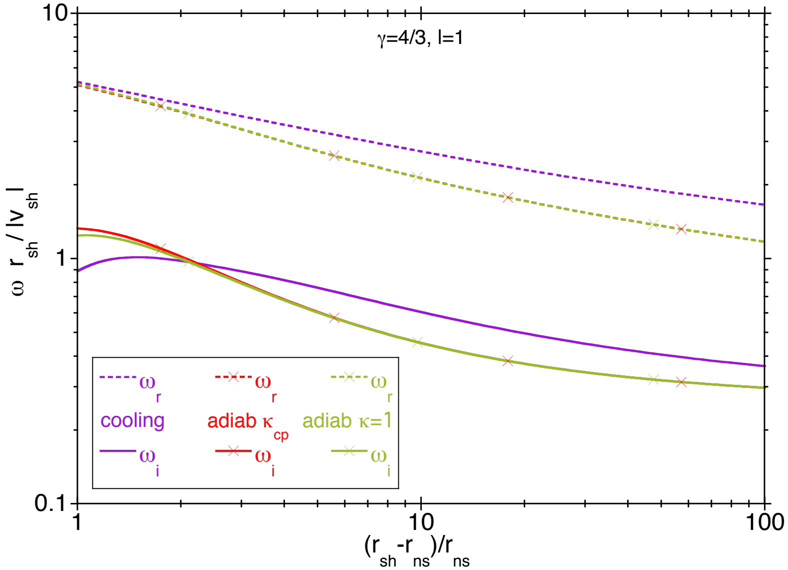

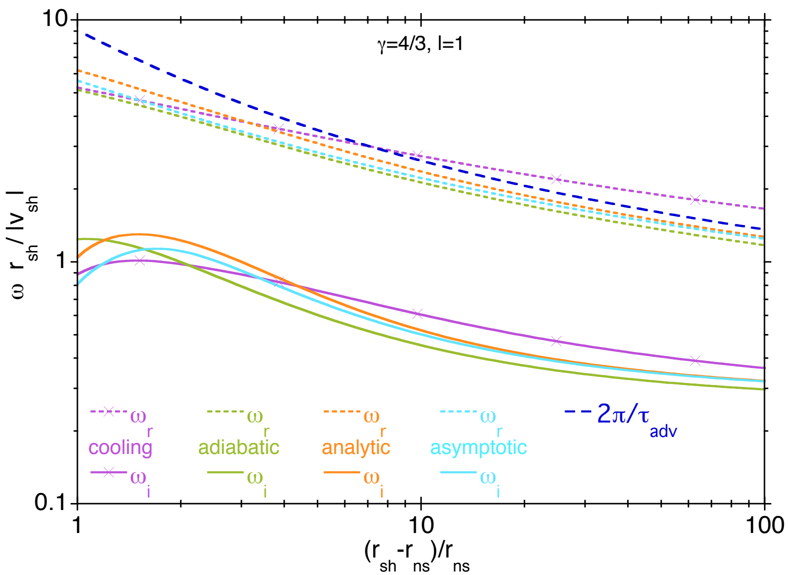

The adiabatic model
captures the main properties
of SASI fundamental mode
regardless of the inner boundary condition

$$\mathcal{Q}(Z) \equiv \frac{2b\left(\frac{r_{\rm sh}}{r_{\rm ns}}\right)^{2-b}\left\{1+\left[(Z+2)^2-b^2\right]\frac{\mathcal{M}_{\rm sh}^2}{l(l+1)x_{\rm sh}^3}\right\}}{\left[1-(Z+2-b)N\right](Z+2+b)-\frac{Z+2-b}{x_{\rm sh}^{2b}}}$$

$$b \equiv [1+l(l+1)]^{\frac{1}{2}}$$

$$N(Z) \equiv \frac{\gamma-1}{b+a}\mathcal{M}_{\rm sh}^2 + \frac{1-\mathcal{M}_{\rm sh}^2-\frac{Z}{b+a}\frac{v_{\rm sh}}{v_1}}{\frac{v_1}{v_{\rm sh}}\frac{1}{2\eta^2}-2+\left(1-\frac{v_{\rm sh}}{v_1}\right)Z},$$

$$d_1 \equiv \frac{1}{2b} - N_{(b-2)}$$

$$\boxed{\begin{aligned} \omega_i &= \frac{\log|\mathcal{Q}|}{\tau_{\rm adv}^{\rm ns}}, \\ \omega_r &= \frac{2n\pi-\varphi_{\mathcal{Q}}}{\tau_{\rm adv}^{\rm ns}}. \end{aligned}}$$

$$\boxed{\zeta \equiv \log\frac{r_{\rm sh}}{r_{\rm ns}}}$$

$$\boxed{|\mathcal{Q}| = \left(\frac{r_{\rm sh}}{r_{\rm ns}}\right)^{2-[1+l(l+1)]^{\frac{1}{2}}} + \mathcal{O}\left(\frac{1}{\zeta^2}\right)}$$

$$\boxed{\varphi_{\mathcal{Q}} = -\frac{2n\pi d_1}{\zeta-d_1} + \mathcal{O}\left(\frac{1}{\zeta^3}\right)}$$

$$\boxed{\frac{\omega_r r_{\rm sh}}{|v_{\rm sh}|} = \frac{2n\pi}{\zeta-d_1} + \mathcal{O}\left(\frac{1}{\zeta^4}\right)}$$

$$\boxed{\omega_i = \frac{\log|\mathcal{Q}|}{\tau_{\rm adv}^{\rm ns}},}$$

SASI oscillations can leave a direct imprint on the gravitational wave and neutrino signals: reverse engineering?

Gravitational Waves

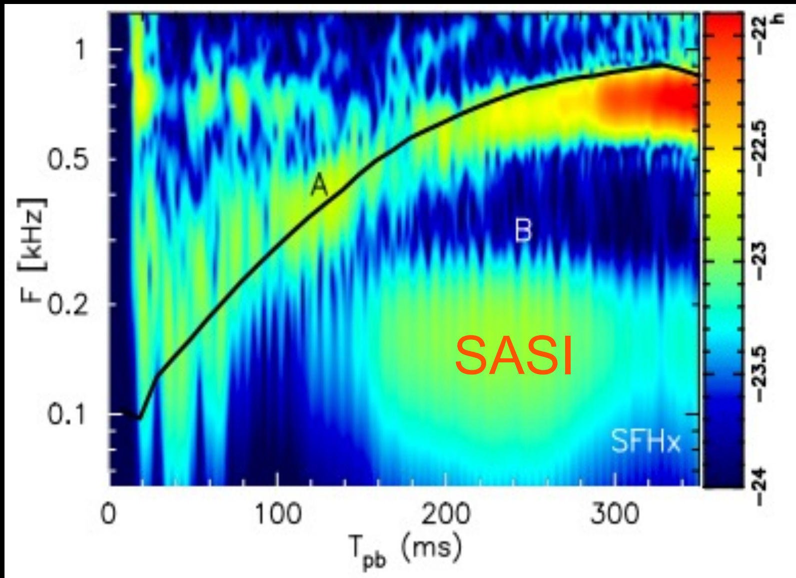

Kuroda+16

Oscillations of the neutrino flux

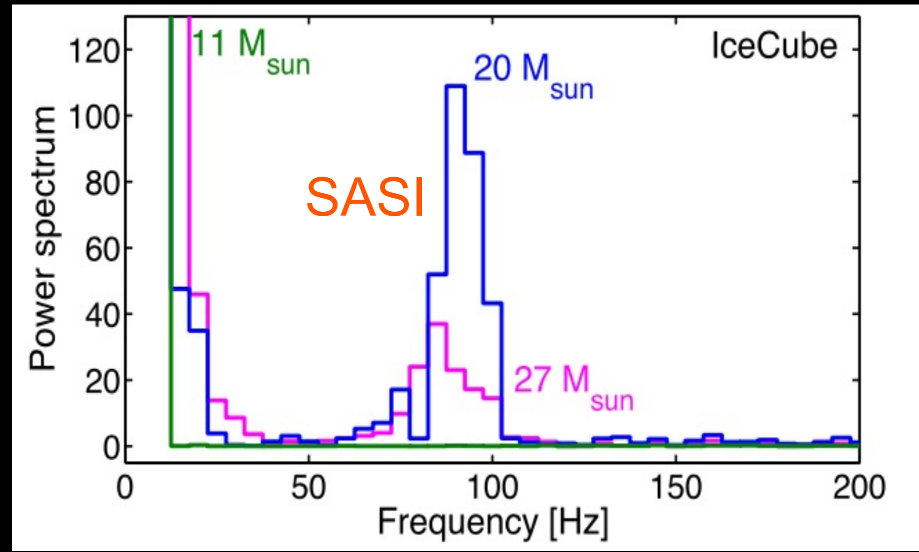

Tamborra+13

Indirect information can also be learnt from

-the kick, spin of the compact object

-the chemical composition of the remnant

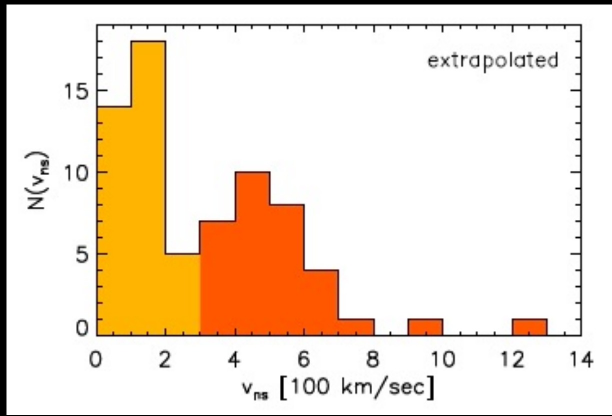

Scheck+06

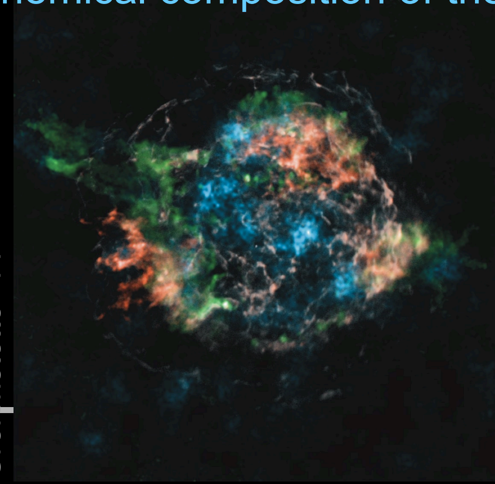

Grefenstette+14

Current and future detectors of neutrinos and gravitational waves